DEVELOPMENT OF FINITE STRAIN VISCOELASTIC-PLASTIC CONSTITUTIVE MODEL

A THESIS

submitted by

ARAVIND PEKETI

for the award of the degree

of

MASTER OF SCIENCE
(by Research)

MACHINE DESIGN SECTION
DEPARTMENT OF MECHANICAL ENGINEERING
INDIAN INSTITUTE OF TECHNOLOGY MADRAS
CHENNAI-600 036

APRIL 2007

Dedicated To

My PARENTS

THESIS CERTIFICATE

This is to certify that the thesis entitled **"DEVELOPMENT OF FINITE STRAIN VISCOELASTIC-PLASTIC CONSTITUTIVE MODEL"** submitted by **ARAVIND PEKETI** to the Indian Institute of Technology Madras, Chennai for the award of the degree of Master of Science (By Research) is a bonafide record of research work carried out by him under our supervision. The contents of this thesis, in full or in parts, have not been submitted and will not be submitted to any other Institute or University for the award of any degree or diploma.

Research Guides

DR. R. KRISHNA KUMAR
Professor – On Sabbatical
Department of Engineering Design
Indian Institute of Technology Madras
Chennai – 600 036
India

DR. T. ASOKAN
Associate Professor - Guide I/C
Department of Engineering Design
Indian Institute of Technology Madras
Chennai – 600 036
India

Chennai- 600 036

Date:

ACKNOWLEDGEMENTS

I express my sincere thanks and profound sense of gratitude to my research guide **Prof. R. Krishna Kumar** for his invaluable guidance, constant encouragement and involvement in my research work. His expertise in different fields always admires me. His approach with the mix of experience, dedication and passion always motivates me. I also thank **Dr. T. Asokan**, my guide I/C, for his invaluable support.

I am thankful to the coordinators of the projects: '**Centre for Finite Element Analysis and Design**' - Prof. R. Krishna Kumar and Prof. A. Meher Prasad and **'Centre of Excellence for Tyre and Vehicle Mechanics**' - Prof. R. Krishna Kumar in which I was employed. The M.S. work would not have been possible without this financial support.

I am thankful to the Director, IIT Madras**,** the Head, Department of Mechanical Engineering, and the Head of Machine Design Section for providing me the necessary facilities and infrastructure to carry out my research work. I am thankful to my GTC members, **Dr. V. Kamakoti,** Department of Computer Science and Engineering, and **Dr. L. Vijayaraghavan,** Department of Mechanical Engineering for their valuable comments and suggestions during various stages of my research work.

I express sincere thanks to **Dr. K. V. Narasimha Rao** for his constant support and suggestions in all matters. It has been great pleasure and rewarding experience working

with him. I am grateful to my friends **Balaram**, **Venkat** and **Subhani** for being a very good company at my lab and for their motivation during hard times. Their affection made me to feel like I am staying in home. I am thankful to my lab mates Guru, Maran, Ravishankar, KrishnaKaran, Gaurav, Vashisht, Sreepada, Raja, Maneesh, Ganesh, Vinid, Bipin who made my research at lab, a nice experience. I am especially thankful to Siva, Jayarao, Nandu, Chandu, Anand, Satya, Prasad, Seshu, Vikas for being a very good friends and company at hostel. I also thank my fellow research scholars Shivraj, Dharmendra, Rahul, Moorthy for being a good company during my courses work.

A special thanks to my friends **Suresh and Gowreeswar,** who supported during toughest phase of my life. I thank my friends, Kumar, Nag, Satish, Koti for giving a good company, during my stay in Chennai. I also thank my classmates at Trichy, Mohan, Murajith, Visakh, Nallasamy for their moral and financial support. I am thankful to bhagini Padmini Rajagopalan, who taught me Yoga and Sanskrit, whose selfless life style impressed me a lot.

Last but not the least, I thank my parents and brother for the great deal of understanding and support they provided to complete my research work. Finally, I express my thanks to all who have helped me during the period of my research work and made my stay at IIT Madras a pleasant and rich experience.

ABSTRACT

KEYWORDS: Finite viscoelasticity, viscoplasticity, mechanical behavior of elastomers, constitutive modeling, return mapping algorithms, multiplicative decomposition

A constitutive model suitable for rubber has been developed in this work. It is based on the multiplicative decomposition of the total deformation gradient into elastic-viscoelastic and elastic-plastic parts. Two independent intermediate configurations one for plasticity and the other for viscoelasticity are assumed. The total stored energy is assumed to be additively decomposed into three parts, elastic, viscoelastic and plastic. Viscous behavior is modeled based on the traditional spring dash pot system. Equilibrium hysteresis is modeled using endochronic theory of plasticity, because equilibrium hysteresis is similar to the rate independent plasticity. The advantage of using endochronic theory of plasticity is that there is no need to assume an yield surface. Since the aim here is to predict the equilibrium hysteresis, endochronic theory seems to be more appropriate. Two evolution equations one for viscous dash pot and the other for plastic dissipation are proposed based on the second law of thermodynamics. Both evolution laws are non linear in nature and Newton-Raphson (N-R) method is used for solution. The state variables for plasticity and viscous behavior are updated using two independent local N-R iterations. Return mapping algorithms in combination with operator split, which are successfully applied in the case of elastoplastic material models with multiplicative decomposition, are used. The predictor-corrector method makes the model

computationally attractive and easy to implement for numerical codes such as finite elements. The material model is implemented in ABAQUS/Standard through UMAT subroutine. Yeoh form is used for all the stored energy functions involved. A procedure for deriving the material constants is discussed. The type of experiments to be conducted in order to achieve material parameters is listed. Material constants are derived and compared with experimental data given in Lion (1996).

TABLE OF CONTENTS

Table of Contents (continued) **Page No.**

Table of Contents (continued) **Page No.**

LIST OF TABLES

LIST OF FIGURES

List of Figures (continued) **Page No.**

ABBREVIATIONS

1-D	One-dimensional
3-D	Three-dimensional
N-R	Newton-Raphson
dof	degrees of freedom

NOTATION

$\tilde{F}$ deformation gradient

$\hat{\tilde{F}}$ volumetric deformation gradient

$\bar{\tilde{F}}$ deviatoric deformation gradient

$\tilde{F}_v$ viscoelastic deformation gradient

$\tilde{F}_{ev}$ elastic-viscoelastic deformation gradient

$\hat{\tilde{F}}_{ev}$ volumetric elastic-viscoelastic deformation gradient

$\bar{\tilde{F}}_{ev}$ deviatoric elastic-viscoelastic deformation gradient

$\tilde{F}_p$ plastic part of the deformation gradient

$\tilde{F}_{ep}$ elastic-plastic deformation gradient

$\hat{\tilde{F}}_{ep}$ volumetric elastic-plastic deformation gradient

$\bar{\tilde{F}}_{ep}$ deviatoric elastic-plastic deformation gradient

$\tilde{C}$ right Cauchy-Green deformation tensor

$\tilde{C}_{ev}$ elastic-viscoelastic right Cauchy-Green deformation tensor

$\tilde{C}_{ep}$ elastic-plastic right Cauchy-Green deformation tensor

$\tilde{C}^{\tau J}$ Jaumann rate of Kirchoff stress

$\tilde{C}^{\sigma T}$ Truesedell rate of Cauchy stress

$\tilde{C}^{\tau}$ spatial tangent moduli

$\tilde{b}$ left Cauchy-Green deformation tensor

Notation (Continued)

$\tilde{b}_{ev}$ elastic-viscoelastic left Cauchy-Green deformation tensor

$\tilde{b}_{ep}$ elastic-plastic left Cauchy-Green deformation tensor

$\hat{\tilde{b}}_{ev}$ volumetric elastic-viscoelastic left Cauchy-Green deformation tensor

$\bar{\tilde{b}}_{ev}$ deviatoric elastic-plastic left Cauchy-Green deformation tensor

$\hat{\tilde{b}}_{ep}$ volumetric elastic-plastic left Cauchy-Green deformation tensor

$\bar{\tilde{b}}_{ep}$ deviatoric elastic-plastic left Cauchy-Green deformation tensor

J determinant of deformation gradient

J_{ev} determinant of elastic-viscoelastic deformation gradient

J_{ep} determinant of elastic-plastic deformation gradient

$\tilde{I}$ identity tensor

$\tilde{H}$ nominal entropy flux

$\bar{R}$ entropy produced by the source per unit time and unit volume

$\tilde{Q}$ Heat Flux

R Heat produced by the source per unit time and unit volume

d_{int} dissipation

d_v viscoelastic part of dissipation

d_p plastic part of dissipation

t time in sec

$\dot{z}$ kinematic arc length

ψ stored energy function per unit volume

Notation (Continued)

ψ_e elastic part of stored energy function

ψ_v viscoelastic part of stored energy function

ψ_p plastic part of stored energy function

ψ_{vol} volumeric part of stored energy function

ψ_{iso} isochoric part of stored energy function

Γ total entropy

$\bar{\eta}$ entropy possessed by body

θ temperature in Kelvin

ε strain

$\tilde{\sigma}$ Cauchy stress tensor

$\tilde{\sigma}_e$ elastic part of Cauchy stress tensor

$\tilde{\sigma}_v$ viscoelastic Cauchy stress tensor

$\tilde{\sigma}_p$ plastic Cauchy stress tensor

η dissipation constant

η_{Dv} deviatoric viscoelastic dissipation parameter

η_{Vv} deviatoric viscoelastic dissipation parameter

η_{Dp} deviatoric plastic dissipation parameter

η_{Vp} deviatoric plastic dissipation parameter

$\tilde{S}$ second-Piola Kirchoff stress tensor

$\tilde{S}_e$ elastic second-Piola Kirchoff stress tensor

$\tilde{S}_v$ viscoelastic second-Piola Kirchoff stress tensor

Notation (Continued)

$\tilde{S}_p$ plastic second-Piola Kirchoff stress tensor

$\tilde{\tau}$ Kirchoff stress tensor

$\tilde{\tau}_e$ elastic Kirchoff stress tensor

$\tilde{\tau}_v$ viscoelastic Kirchoff stress tensor

$\tilde{\tau}_p$ plastic Kirchoff stress tensor

$\tilde{\gamma}_v$ viscoelastic fourth order isotropic tensor

$\tilde{\gamma}_p$ plastic fourth order isotropic tensor

λ_{ev} eigen values of elastic-viscoelastic deformation gradient

λ_{ep} eigen values of elastic-plastic deformation gradient

CHAPTER 1

CONSTITUTIVE MODELLING

1.1 INTRODUCTION

Rubber is an important material in many applications such as automobile tires, damping devices etc. In many cases rubber components are subjected to complex loading. Such complex loading give raise to a number of research issues. One such issue in the tire industry is the rolling resistance, which is due to the loading / unloading sequence of the tire.

Mechanical properties of elastomers have been one of the most important research area. According to Treloar (1975), rubber can be considered as a sub class of a wider chemical group of elastomers.

Mechanically, the important property that distinguishes rubber from other common materials such as metals is its ability to dissipate energy. In earlier days rubber is considered only as an elastic material, which can take large deformation before its failure. With the development of experimental facilities, rubber is established as a viscoelastic material which has a rate dependent deformation behavior. In addition to its ability to dissipate energy, rubber can also go through large range of deformations, before it fails to

deliver the intended purpose. Depending on the type of rubber the maximum strain it can sustain may go up to 1000% (Reese and Wriggers, 1997).

A major consumer of rubber today is the tire industry. One of the main functions of the automobile tire is to absorb the small scale vibrations that arise due to road conditions. Till today, there is no alternative material for rubber to match good damping characteristics, ability to sustain large deformations, ability to undergo large numbers of loading / unloading cycles without failure, and most importantly at reasonable cost. In case of tires, the hysteresis of rubber gives rise to what is known as rolling resistance. In a typical passenger car tires rolling resistance accounts for approximately 15% of the fuel consumed (Narasimharao, 2005). Its prediction depends on a proper constitutive viscoelastic model. Hence a constitutive model which accurately predicts the deformation behavior of rubber is of great importance in tire industry as well as in other industries, where rubber is the prime ingredient.

Recent experimental investigations on the deformation behavior of rubber show a strong rate dependency along with the so called equilibrium hysteresis (Haupt and Sedlan, 2001). Hence for any constitutive model to represent the true nature of rubber, it should include non linear elasticity, rate dependencies and rate independent hysteresis (Lion, 1997a). According to Haupt (2000), mechanical material behavior can be classified into four categories, as shown in Figure. 1.1.

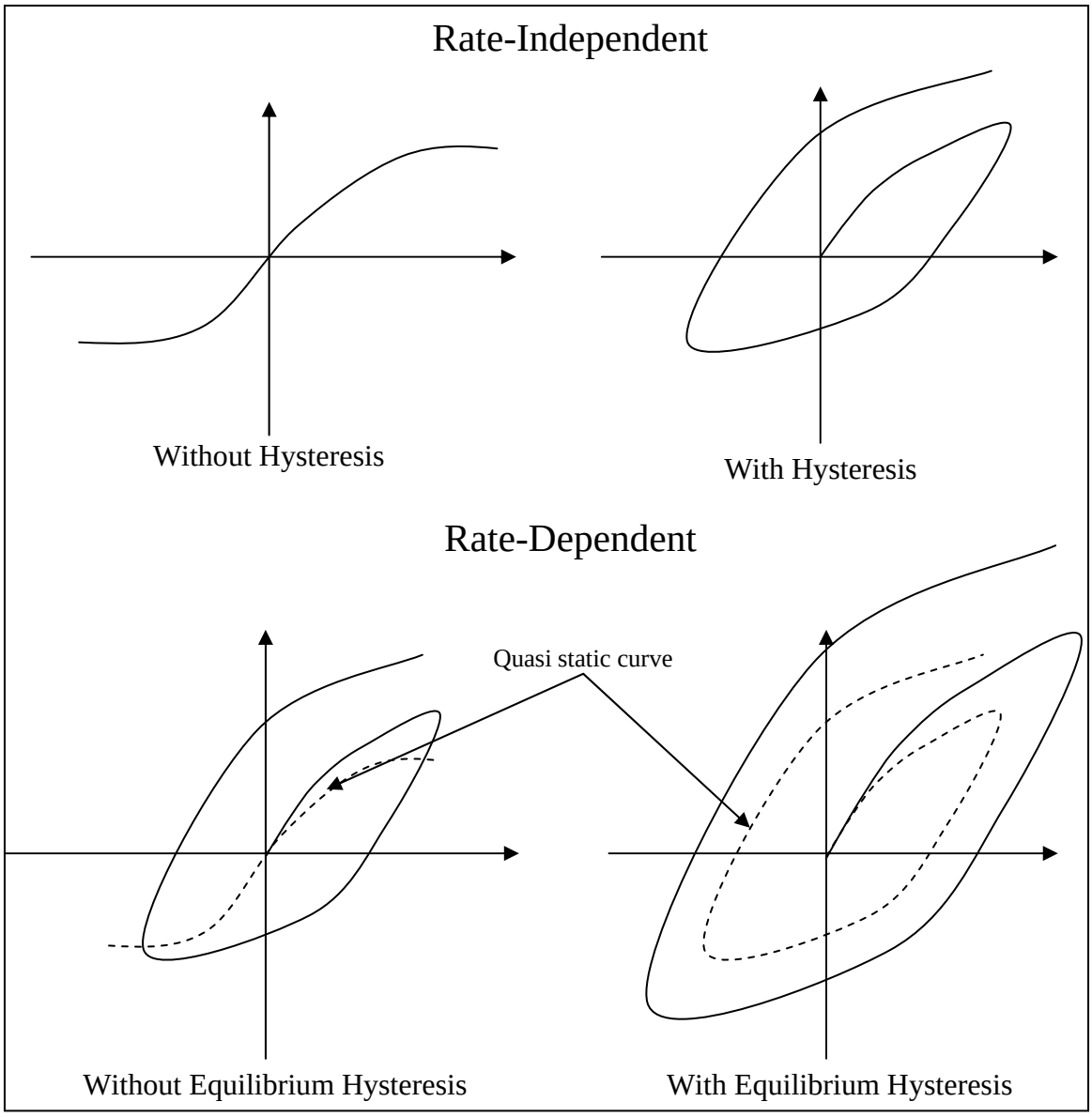

Fig. 1.1 Classification of Mechanical Behavior of Materials (Haupt, 2000)

1.2 FINITE DEFORMATION MECHANICS

If the material is expected to have high strain ranges, the general small deformation theory is not applicable and a whole new set of definitions for deformation, strain and stress measures have to be used. To this end concepts from continuum mechanics are

used. The following are the most general terms used in finite deformation mechanics defined here for completeness (Holzapfel, 2000).

1.2.1 Deformation gradient

Deformation gradient gives the relationship between an initial or reference configuration and the deformed configuration. An initial configuration is the position in space occupied by a body before the application of loads as shown in Figure 1.2. Under Lagrangian frame initial and the reference configuration are one and the same. A deformed configuration of a body is the position in space occupied by a body after the application of forces. If $d\tilde{X}$ is the infinitesimal line element in the reference configuration and same line element is deformed to $d\tilde{x}$ after the application of loads, the deformation gradient $\tilde{F}$ gives the relation ship between $d\tilde{X}$ and $d\tilde{x}$

$$dx_i = \frac{\partial x_i}{\partial X_J} dX_J \tag{1.1}$$

$$F_{iJ} = \frac{\partial x_i}{\partial X_J} \tag{1.2}$$

From Equation 1.2 it can be observed that $\tilde{F}$ is a two point tensor involving point in reference configuration as well as deformed configuration. Also $d\tilde{X}$ defines the linear transformation which relates $d\tilde{x}$ in deformed configuration to $d\tilde{X}$ in reference configuration. It is worth noting that $d\tilde{X}$ also includes rigid body motion of the body.

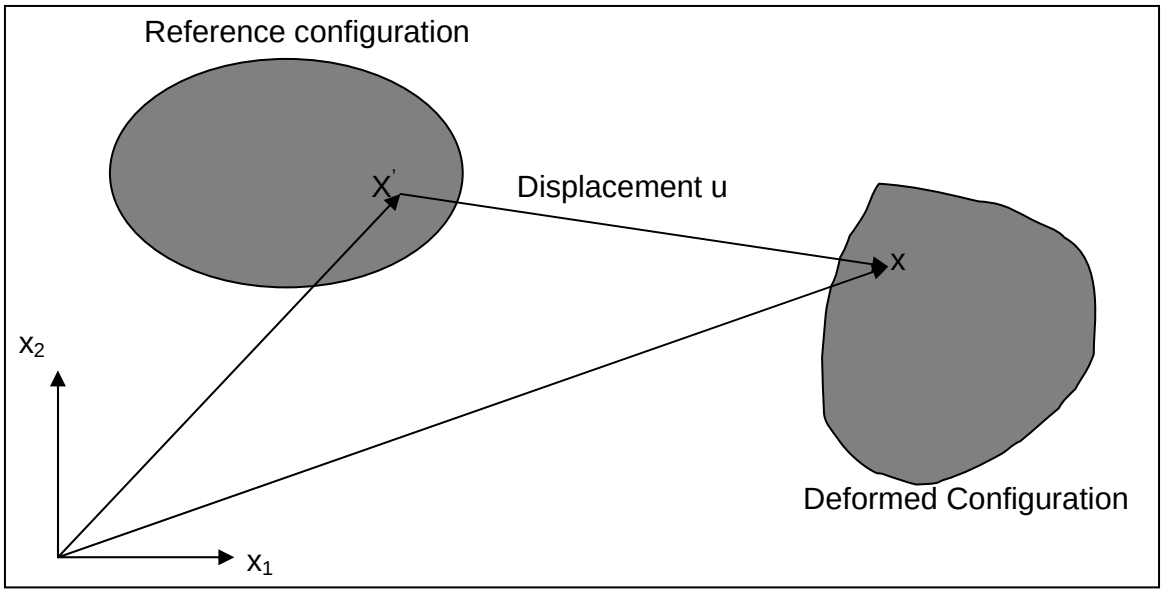

Fig. 1.2 Reference and Deformed Configurations of a Body

1.2.2 Strain tensors

There are two most important deformation tensors through which most of the strain measures are defined. The first one is called right Cauchy-Green deformation tensor or Green deformation tensor $\tilde{C}$ defined through Equation 1.3 and the left Cauchy-Green deformation tensor or finger deformation tensor $\tilde{b}$ defined through Equation 1.4. In general $\tilde{C}$ is used when the strain definition is in material co-ordinates and $\tilde{b}$ in the spatial co-ordinates.

$$\tilde{C} = \tilde{F}^T \tilde{F} \tag{1.3}$$

$$\tilde{b} = \tilde{F}\tilde{F}^T \tag{1.4}$$

One of the important features of both $\tilde{C}$ and $\tilde{b}$ is that they are symmetric.

1.2.3 Push-forward and pull-back operations

A push-forward is an operation in which a vector or tensor under the reference configuration is transformed to deformed or current configuration. A pull-back is an operation in which a vector or tensor under the current configuration is transformed to reference configuration. These are very useful operations used for example in Lie time derivative, in which the tensor under consideration is subjected to a pull-back to reference configuration, where material time derivative is calculated and then push-forwarded to current configuration.

1.2.4 The second law of thermodynamics for continuum

This is perhaps the most important law governing any constitutive model. The constitutive model should satisfy the second law of thermodynamics which is also known as entropy inequality principle. It states that 'the total entropy production for all thermodynamic processes is never negative'.

$$\Gamma(t) = \frac{D}{Dt}\int_{\Omega_0} \bar{\eta}\left(X,t\right) dV + \int_{\partial\Omega_0} \tilde{H}\cdot\tilde{N}\, dS - \int_{\Omega_0} \bar{R}\, dV \geq 0 \tag{1.5}$$

In the Equation 1.5, $\Gamma(t)$ denotes the total production of entropy, $\bar{\eta}\left(X,t\right)$ is the entropy possessed by the body, $\tilde{H}\left(X,t\right)$ is the nominal entropy flux defined per unit reference surface area and $\bar{R}$ is the entropy produced by the source per unit time and unit reference volume.

1.2.4.1 Clausius-Duhem inequality

Assuming that entropy input is related to rate of thermal work, and the entropy flux $\tilde{H}$ and the entropy source $\bar{R}$ are related to heat flux $\tilde{Q}$ and heat source R, the Clausius-Duhem inequality can be written as

$$\Gamma(t)=\frac{D}{Dt}\int_{\Omega_0}\bar{\eta}\left(x,t\right)dV+\int_{\partial\Omega_0}\frac{\tilde{Q}}{\theta}\cdot\tilde{N}\,dS-\int_{\Omega_0}\frac{R}{\theta}dV\geq 0 \tag{1.6}$$

In Equation 1.6 it is postulated that

$$\tilde{H}=\frac{\tilde{Q}}{\theta}\ ,\ \bar{R}=\frac{R}{\theta} \tag{1.7}$$

In the Equation 1.7 $\tilde{Q}$ is the heat flux and R is the heat produced by the source. Converting the surface integral in Equation 1.6 to volume integral and using the fact that the reference volume V is independent of time, the Clausius-Duhem inequality under material co-ordinates can be written as

$$\dot{\bar{\eta}}-\frac{R}{\theta}+\frac{1}{\theta}Div\tilde{Q}-\frac{1}{\theta^2}\tilde{Q}.Grad\theta\geq 0 \tag{1.8}$$

From the energy balance equation, eliminating the heat source R

$$\tilde{P}:\dot{\tilde{F}}-\dot{e}+\theta\dot{\eta}-\frac{1}{\theta}\tilde{Q}.Grad\theta\geq 0 \tag{1.9}$$

In the Equation 1.9 the first term gives the stress power, which gives the rate of internal mechanical work, alternative forms of stress power can be used depending on the stress measure and the configuration under consideration.

1.3 ENDOCHRONIC THEORY OF PLASTICITY

Endochronic theory of plasticity is originally introduced by Valanis (1971). The main feature that differentiates this theory from the classical theory of plasticity is that there is no concept of yield surface. It is originally developed for metals such as aluminum, brass etc. in which it is difficult to distinguish the starting point of yield on the stress strain curve. Valanis (1971) used thermodynamic internal state variables along with intrinsic time scale to represent the plastic deformation. This theory has many advantages compared to flow theory of plasticity e.g. simplicity in calculations and can represent the typical metal behaviors such as Bauschinger effect. Using his theory Valanis (1980) showed that the flow theory plasticity can be derived from endochronic theory.

1.4 PRACTICAL APPLICATIONS: ROLLING RESISTANCE OF TIRE

The dissipation behavior of the rubber is important in many cases as described in previous sections, here rolling resistance of the tire is briefed to understand importance of the dissipation behavior of rubber. In simple terms the rolling resistance of a tire is nothing but the energy required to maintain the rolling motion of the tire. Consider a wheel rolling freely on a flat surface. If both the wheel and the road were perfectly rigid, and no friction exists between the road and the wheel, there would be no resistance and consequently no need to exert a tractive force. In real world however perfect rigid bodies do not exist and both the road and the wheel are subjected to deformation in the contact zone: To produce this deformation it is necessary to spend some energy which is not

completely recovered at the end of contact zone. This energy dissipation is what causes the rolling resistance (Genta, 1997). While the rolling resistance is mainly due to the dissipative nature of the materials in the deformation zone, other small factors such as sliding between road and wheel, aerodynamic drag and friction in the wheel hub also contribute to it. This dissipated energy is converted into heat and convected to the surroundings. The distribution of the contact pressure, which is symmetric with respect to the vertical axis under static conditions, becomes unsymmetric because of which the normal force shifts its axis of application from the centre of contact patch as shown in Figure 1.3. The rolling resistance is as a result of this shift in resultant force producing torque.

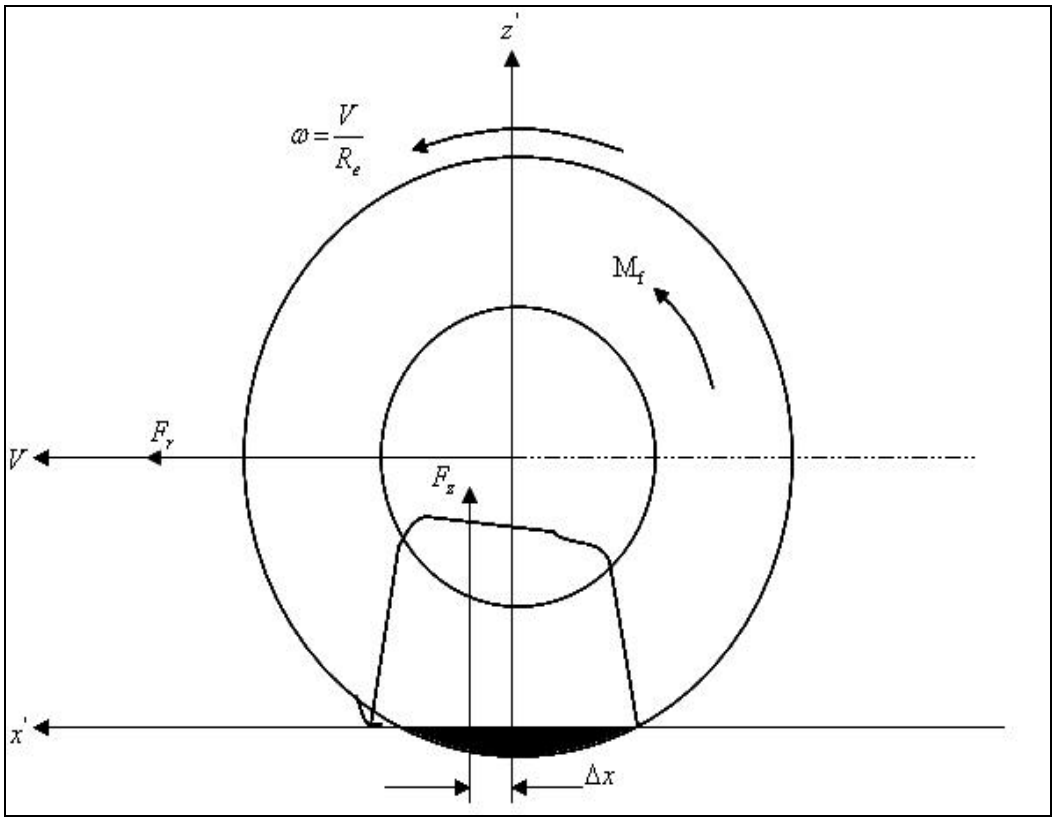

Fig. 1.3 Rolling Resistance of a Tire

An estimate of dissipation of the energy gives a good first hand understanding of the amount of rolling resistance in a tire, as it is the prime contributor to it. A small contribution is made at the tire road interface. To this end, the material model should be able to represent the dissipation characteristics of the material accurately. In a typical passenger car tire, nearly twelve different materials are used. Figure 1.4 shows the different regions of typical passenger car tire. Almost all of them are dissipative in nature.

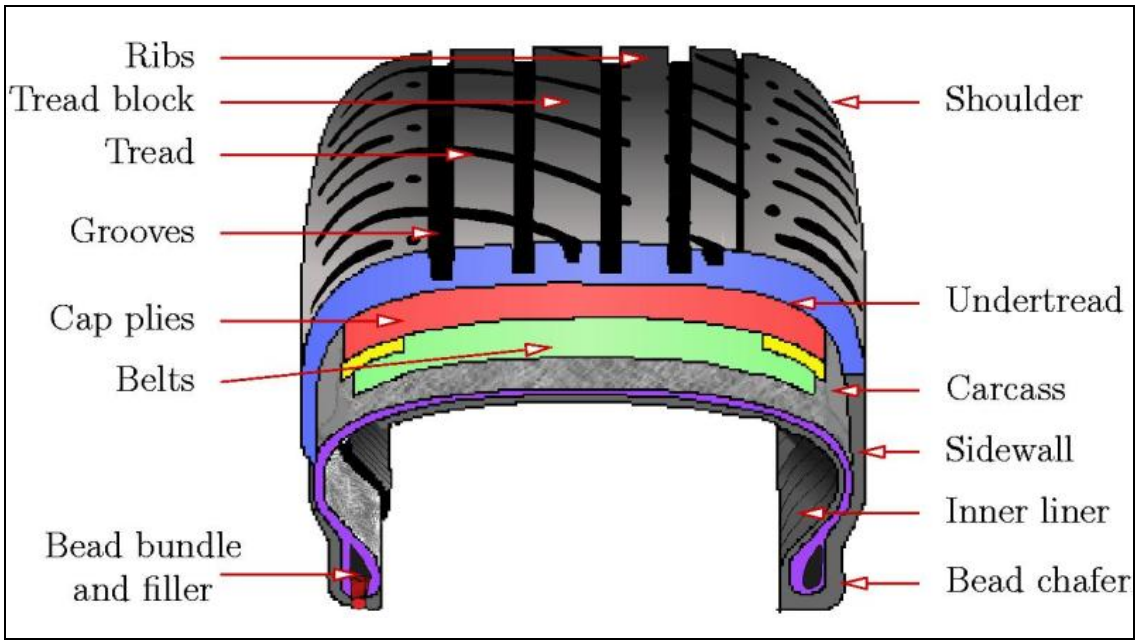

Fig. 1.4 Cross Section of a Typical Passenger Car Tire Showing Different Regions (http://www2.eng.cam.ac.uk)

Figure 1.5 shows the contribution to the dissipation from various parts of the tire. The study was done by Narasimha Rao(Narasimha Rao, 2005). The figure shows the approximate percentage of total dissipation in each of the tire materials for 235/75R15 passenger car radial. The analysis was performed at 40 kmph rolling speed, 210 kPa of

inflation pressure and load on tyre is 6kN. The tread material is the significant contributor to the rolling resistance with 55%.

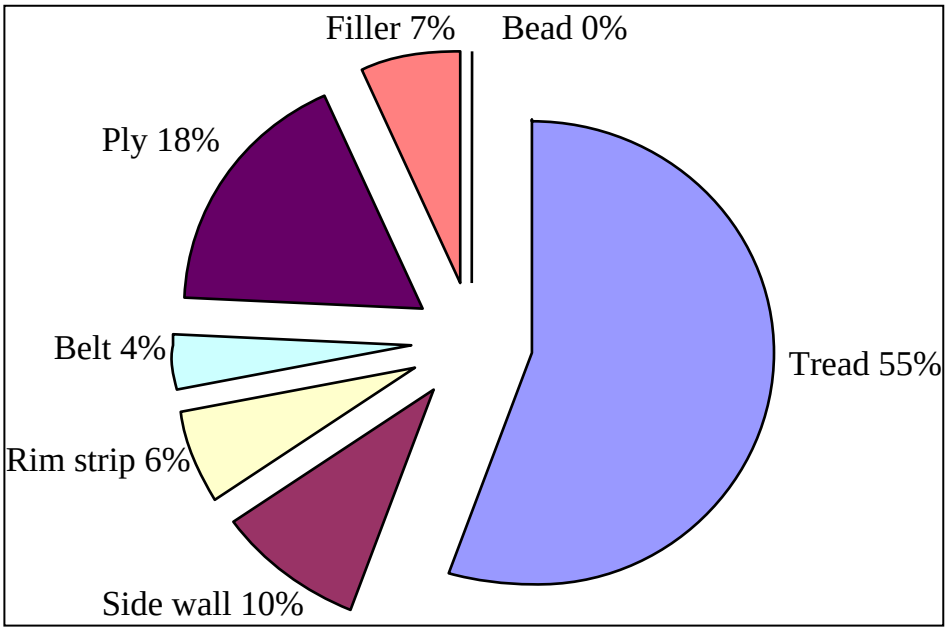

Fig. 1.5 Dissipation at Different Tire Regions Under Normal Operating Conditions (Narasimharao, 2005)

1.5 LITERATURE SURVEY

Traditionally rubber is considered as a hyperelastic material with a specific strain energy density function or stored energy function. Well known forms of strain energy density function include Mooney (Treloar, 1975), Ogden (Ogden, 1972), Yeoh (Yeoh, 1993) etc. While the hyperelastic approach to model rubber is phenomenological in nature, many attempts have been made to derive their behavior using statistical mechanics (Treloar, 1975). The advantage of the micromechanical models is that they can represent the

deformation behavior accurately and the disadvantage is that it is very difficult to use them to solve practical problems.

It is well known that the rubber shows what is known as rate dependency, also refereed to as hysteresis (Haupt and Sedlan, 2000). The fundamental models of viscoelasticity such as Maxwell model and the Kelvin-Voigt model are valid only for the linear range, close to the thermodynamic equilibrium, and go by the name linear viscoelastic models. Many applications require the models to be non-linear elastic in nature. A number of viscoelastic material models suitable for rubber like materials were proposed e.g. Arruda and Boyce (1993), Bergstorm and Boyce (1998), Bonet (2001), Drozdov (1997), Haupt and Lion (2002), Holzapfel (1996), Lubliner (1985), Le Tallec *et al.*(1993) among others. Of the above models Arruda and Boyce (1993) proposed a eight-chain model based on the non-Gaussian behavior of the individual chains, Bergstorm and Boyce (1998) conducted experiments on filled and natural rubbers and proposed a constitutive model based on the multiplicative decomposition of the deformation gradient and Drozdov (1997) employed fractional derivatives of tensor functions for the constitutive model.

An extension of the small strain approach to large strain viscoelasticity results in what is known as finite linear viscoelastic models. One such model suitable for fiber reinforced material has been proposed by Kaliske (2000). Reese and Govindjee (1998a) have developed a finite non linear viscoelastic constitutive model for large deformations and large deviations away from thermodynamic equilibrium which is consistent with the second law of thermodynamics and uses multiplicative decomposition of the deformation

gradient. But their model does not include the equilibrium hysteresis. Reese and Govindjee (1998b) have proposed a thermo-viscoelastic constitutive model using a non linear evolution law to include thermal effects. The computational setting is also addressed and they have used predictor-corrector algorithm to integrate the evolution equations.

Very recent models proposed by Haupt and Sedlan (2001), Lion (1997b, 1998), Lin and Schomburg (2003), Nedjar (2000b) consider viscoplasticity which include rate dependent and the so called rate independent hysteresis. Lion (1996) has suggested a viscoplastic constitutive model using an additive decomposition of the total stress into a rate independent equilibrium stress and a rate dependent overstress within the framework of dual variables. He has investigated the temperature effects on the mechanical properties of a filled-loaded rubber experimentally, and described a physically based method to represent its behavior. He used multiplicative decomposition of the total deformation gradient into mechanical and thermal parts. Lin and Schomburg (2003) have proposed a finite elastic-viscoelastic-elastoplastic constitutive model for rubber like materials including Mullins effect. Their model is based on the multiplicative decomposition of the deformation gradient and is derived using objective rates for calculating time derivatives.

In contrast to the above models, Reese and Wriggers (1997), neglected the rate dependent behavior of rubber-like polymers and proposed a elastic-plastic material model using multiplicative decomposition of the deformation gradient and internal state strain like variables for modeling plasticity along with von-Mises yield criterion.

The other inelastic effect observed in rubber like polymers is Mullins effect (Mullins, 1948; Beuche, 1959; Mullins, 1969), which is characterized as strain induced softening and persists only during initial cycles of deformation. Govindjee and Simo (1991) have proposed a damage model for incorporating Mullins effect from the micromechanical point of view. Govindjee and Simo (1992) extended the micromechanical model to phenomenological model for efficient implementation under numerical schemes.

Simo (1992) has studied in detail the return mapping algorithm for finite elasto-plasticity from a computational point of view and his work uses principle of maximum dissipation.

1.6 MOTIVATION

According Narasimha Rao *et al.* (2006), use of existing linear viscoelastic models are not sufficient to predict the experimental findings, warranting a non linear viscoelastic model for the simulation studies. There are many constitutive models proposed in the literature for rubber and viscoplasticity (Lion, 1996; Haupt and Sedlan, 2001; Lin and Schomburg, 2003). There are three key issues in developing a constitutive model. The first is the parameter identification and measurement, the second is the ease of numerical implementation and the third is the computational efficiency. One finds that, a procedure for determining the material parameters is hardly addressed in many of the theoretical studies.

1.7 OBJECTIVES AND SCOPE

The main objectives of the study are:

1. Propose a constitutive model that takes care of the rate dependency, quasi static non linear elastic behavior and hysteresis and be consistent with the second law of thermodynamics.
2. Implement the developed constitutive model in a Finite Element Code and to study its behavior under different test conditions.
3. Develop a procedure for deriving material constants from the experimental data.

The scope of the current work is to achieve the above objectives with the available experimental data in literature. In the process the following assumptions have been made.

1. The material is assumed to be isotropic and homogeneous.
2. The temperature effects are not included i.e. the material properties are assumed to be independent of temperature
3. Mullins effect is not included and it is assumed that the material is pretreated to remove the Mullins effect.

1.8 ORGANIZATION OF THE THESIS

The thesis deals with the development of a finite non linear viscoelastic-plastic material model. A constitutive model based on the second law of thermodynamics is derived and it is implemented under numerical scheme.

Chapter 1 gives a general introduction to the rubber and constitutive modeling with experimental facts. The importance of constitutive modeling of rubber is discussed for practical cases such as rolling resistance. A brief introduction to the general terms in finite deformation mechanics is also presented. This is followed by a list of objectives for the proposed work.

Chapter 2 starts with a one dimensional (1-D) representation of the constitutive model. Later it is generalized to a three dimensional (3-D) setting assuming multiplicative decomposition of the deformation gradient and additive split of the total stored energy. The model is compared with the available models in literature. The algorithmic implementation of the developed model is discussed.

Chapter 3 provides a brief introduction to implement the constitutive model through UMAT subroutine in ABAQUS/Standard. The tangent modulus which is to be updated to ABAQUS through UMAT is derived. Complete algorithm for UMAT is stated step by step.

In Chapter 4, the developed constitutive model is studied for various basic deformation characteristics. It also gives a general procedure to derive the material constants. Material constants were fitted for the available experimental data, using the developed procedure.

In Chapter 5, the conclusions based on the current work are presented. The scope for future work is also stated.

Appendix A provides the complete derivations for the expressions used while developing the constitutive relations.

CHAPTER 2

VISCOELASTIC-PLASTIC CONSTITUTIVE MODEL

2.1 INTRODUCTION

In this chapter a constitutive model is proposed which is suitable for elastomers and includes all the observed deformation behaviors as described in chapter 1. Initially a 1-D small strain representation of the constitutive model is presented and then it will be generalized for the three dimensional case.

2.2 1-D REPRESENTATION OF THE CONSTITUTIVE MODEL

Figure 2.1 shows the 1-D viscoelastic – plastic rheological model as proposed by Lion (1997b). It has three springs in parallel, the top and bottom springs has dissipation elements in series. Dashpot attached to the spring at the bottom characterizes the rate dependent behavior. Dissipation element attached to the top spring characterizes the equilibrium hysteresis. The springs can be non-linear in general. The small strain theory given below follows closely Lion (1997b). The other references include Lin and Schomburg (2003), Reese and Govindjee (1998a). But there are some differences in the form of the equations used in this work when compared to that given in these references. They are highlighted appropriately. Let ε be the total strain and let this total strain be

additively decomposed into $\varepsilon_v, \varepsilon_{ev}$ and $\varepsilon_p, \varepsilon_{ep}$. ε_v is the representative strain in the viscous dashpot and ε_p is the stain in the plastic dissipation element.

$$\varepsilon = \varepsilon_v + \varepsilon_{ev} \tag{2.1a}$$

$$\varepsilon = \varepsilon_p + \varepsilon_{ep} \tag{2.1b}$$

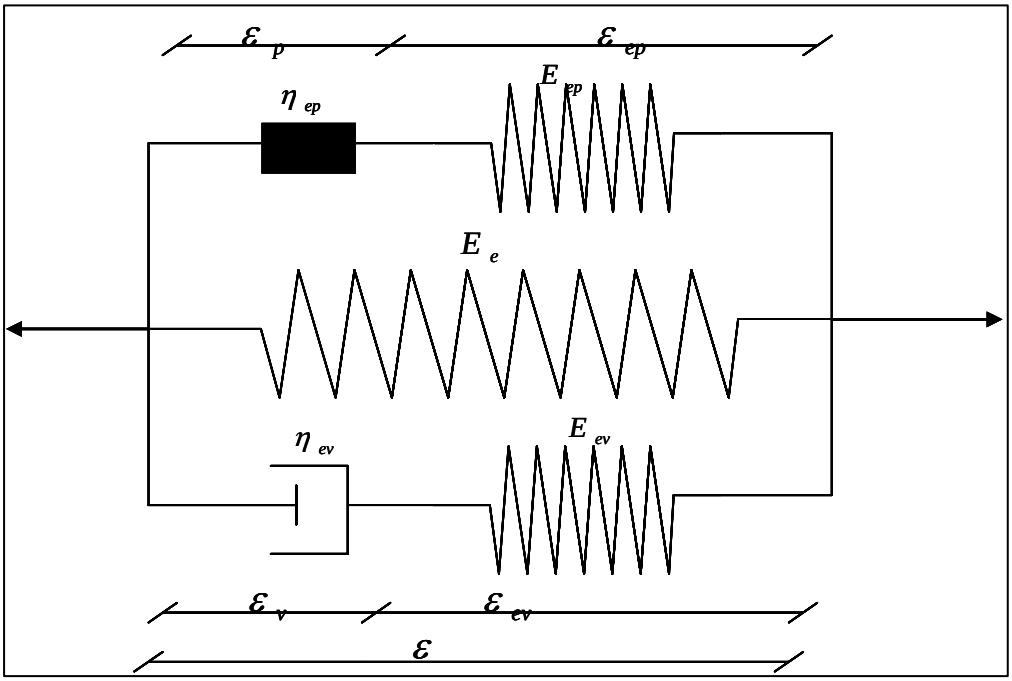

Fig. 2.1 1-D Representation of the Viscoelastic-Plastic Material Model (Lion, 1997b)

The total stored energy is also assumed to be additively decomposed into elastic, viscoelastic and plastic parts as shown below Lion (1997b).

$$\psi = \psi_e\left(\varepsilon_e\right) + \psi_p\left(\varepsilon_{ep}\right) + \psi_v\left(\varepsilon_{ev}\right) \tag{2.2}$$

Where, ψ is the total stored energy.

The second law of thermodynamics in the form of dissipation inequality is given by

$$d_{\text{int}} = \sigma : \dot{\varepsilon} - \dot{\psi} + \bar{\eta}\,\dot{\theta} \geq 0 \tag{2.3}$$

In the Equation 2.3 first term represent the stress power, second term is the rate of change of free energy and third term is the dissipation due to is the entropy change.

Neglecting the temperature effects the dissipation inequality reduces to

$$d_{\text{int}} = \sigma : \dot{\varepsilon} - \dot{\psi} \geq 0 \tag{2.4}$$

Substituting for ψ in the above equation

$$d_{\text{int}} = \left(\sigma - \frac{\partial \psi_e}{\partial \varepsilon} - \frac{\partial \psi_v}{\partial \varepsilon} - \frac{\partial \psi_p}{\partial \varepsilon} \right) \dot{\varepsilon} - \frac{\partial \psi_v}{\partial \varepsilon_v} \dot{\varepsilon}_v - \frac{\partial \psi_p}{\partial \varepsilon_p} \dot{\varepsilon}_p \geq 0 \tag{2.5}$$

From Coleman-Noll condition (Coleman and Gurtin, 1967) $\frac{\partial \psi_e}{\partial \varepsilon_e} = \sigma_e$, $\frac{\partial \psi_v}{\partial \varepsilon} = \sigma_v$, $\frac{\partial \psi_p}{\partial \varepsilon} = \sigma_p$ the total stress σ can be written as

$$\sigma = \sigma_e + \sigma_p + \sigma_v \tag{2.6}$$

Which means, the total stress is also additively decomposed in the same way as that of the stored energy. Hence,

$$d_{\text{int}} = -\frac{\partial \psi_{ev}}{\partial \varepsilon_v} \dot{\varepsilon}_v - \frac{\partial \psi_{ep}}{\partial \varepsilon_p} \dot{\varepsilon}_p \geq 0 \tag{2.7}$$

One way of making the above equation to be positive definite is by making the two terms in the equation individually positive. Now splitting the dissipation inequality into viscoelastic and equilibrium plastic parts

$$\left(d_{\text{int}}\right)_{vis} = -\frac{\partial \psi_v}{\partial \varepsilon_v} \dot{\varepsilon}_v \geq 0 \tag{2.8}$$

$$\left(d_{\text{int}}\right)_{ep} = -\frac{\partial \psi_p}{\partial \varepsilon_p} \dot{\varepsilon}_p \geq 0 \tag{2.9}$$

To make the above equations positive definite Reese and Govindjee (1998a) suggested a form given in Equation 2.10. Here the same equation for the viscoelastic part is adopted from his work. On the other hand, the viscoplastic evolution equation can be written in the Valanis form, as suggested by Lion (1997b). His equation given below becomes cumbersome for numerical implementation.

$$\dot{\varepsilon}_v = -\frac{1}{\eta_v} : \frac{\partial \psi_v}{\partial \varepsilon_v} \tag{2.10}$$

$$\dot{\varepsilon}_p = -\dot{z}\frac{1}{\eta_p} : \frac{\partial \psi_p}{\partial \varepsilon_p} \tag{2.11}$$

In the above equations η_v, η_p are damping coefficients of viscoelastic and plastic dissipation elements and $\dot{z}$ is the kinematic arc length. Equation 2.11 is simple in form and is consistent with Equation 2.10. By proposing evolution equations in the form shown in Equations 2.10 and 2.11, the dissipation inequality is satisfied for arbitrary deformation processes.

2.3 DESCRIPTION OF THE CONSTITUTIVE MODEL

Generalizing the 1-D model is based on the multiplicative decomposition (Lee, 1961; Lubliner, 1985) of the total deformation gradient into two parts, namely elastic-viscoelastic and elastic-equilibrium plastic parts, given by

$$\tilde{F} = \tilde{F}_{ev}\tilde{F}_v \tag{2.12a}$$

$$\tilde{F} = \tilde{F}_{ep}\tilde{F}_{p} \tag{2.12b}$$

The schematic representation of the multiplicative decomposition is shown in the Figure 2.2. It is worthwhile to note that the intermediate configuration defined by the multiplicative decomposition of the total deformation gradient is purely imaginary. Similar decomposition of the deformation gradient has been used by many researchers e.g. Lion (1997b), Lin and Schomburg (2003).

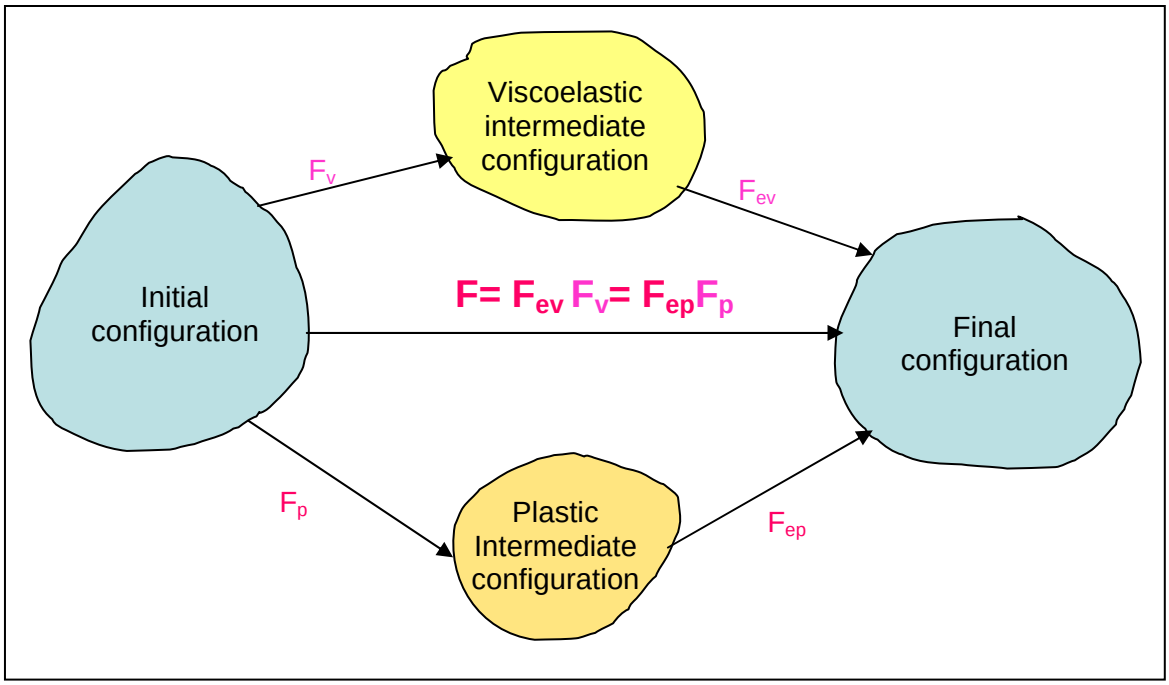

Fig. 2.2 Pictorial Representation of the Multiplicative Decomposition of the Total Deformation Gradient

The total stored energy is assumed to be additively decomposed into three parts as discussed in the 1-D representation and followed by Lion (1996), Reese and Govindjee (1998a)

$$\psi = \psi(\tilde{C}, \tilde{F}_{ev}, \tilde{F}_{ep}) = \psi_e(\tilde{C}) + \psi_v(\tilde{C}_{ev}) + \psi_p(\tilde{C}_{ep}) \tag{2.13}$$

Where $\tilde{C}$ is the right Cauchy deformation tensor defined as

$$\tilde{C} = \tilde{F}^T \tilde{F} \tag{2.14}$$

In the similar way $\tilde{C}_{ev}, \tilde{C}_{ep}$ are defined as

$$\tilde{C}_{ev} = \tilde{F}_{ev}^T \tilde{F}_{ev} = \tilde{F}_v^{-T} \tilde{C} \tilde{F}_v^{-1} \tag{2.15}$$

$$\tilde{C}_{ep} = \tilde{F}_{ep}^T \tilde{F}_{ep} = \tilde{F}_p^{-T} \tilde{C} \tilde{F}_p^{-1} \tag{2.16}$$

From the above definitions it can be observed that $\tilde{C}_{ev}, \tilde{C}_{ep}$ are nothing but the push-forward of the right Cauchy deformation tensor to the corresponding intermediate configurations defined by $\tilde{F}_v$ and $\tilde{F}_p$.

All constitutive equations have to be consistent with the Second law of Thermodynamics, stated as the Clausius – Duhem inequality. After all, one of the popular definitions for an elastic material is based on zero dissipation.

Starting with the Clausius-Duhem inequality (Holzapfel, 2000),

$$\frac{1}{2} \tilde{S} : \dot{\tilde{C}} - \dot{\psi} \geq 0 \tag{2.17}$$

Substituting for ψ in the above equation

$$\left(\tilde{S} - 2 \frac{\partial \psi_e}{\partial \tilde{C}} - 2 \tilde{F}_v^{-1} \frac{\partial \psi_v}{\partial \tilde{C}_{ev}} \tilde{F}_v^{-T} - 2 \tilde{F}_p^{-1} \frac{\partial \psi_p}{\partial \tilde{C}_{ep}} \tilde{F}_p^{-T} \right) : \frac{1}{2} \dot{\tilde{C}} - \frac{\partial \psi_v}{\partial \tilde{C}_{ev}} \frac{\partial \tilde{C}_{ev}}{\partial \tilde{F}_v} : \dot{\tilde{F}}_v - \frac{\partial \psi_p}{\partial \tilde{C}_{ep}} \frac{\partial \tilde{C}_{ep}}{\partial \tilde{F}_p} : \dot{\tilde{F}}_p \geq 0 \tag{2.18}$$

From Coleman and Gurtin (1967) it can be concluded that,

$$\tilde{S} = 2 \frac{\partial \psi_e}{\partial \tilde{C}} + 2 \tilde{F}_v^{-1} \frac{\partial \psi_v}{\partial \tilde{C}_{ev}} \tilde{F}_v^{-T} + 2 \tilde{F}_p^{-1} \frac{\partial \psi_p}{\partial \tilde{C}_{ep}} \tilde{F}_p^{-T} = 2 \frac{\partial \psi}{\partial \tilde{C}} \tag{2.19}$$

Following Reese and Govindjee (1998a), writing $\tilde{S}_e = 2\dfrac{\partial \psi_e}{\partial \tilde{C}}$, $\tilde{S}_v = 2\tilde{F}_v^{-1}\dfrac{\partial \psi_v}{\partial \tilde{C}_{ev}}\tilde{F}_v^{-T}$ and $\tilde{S}_p = 2\tilde{F}_p^{-1}\dfrac{\partial \psi_p}{\partial \tilde{C}_{ep}}\tilde{F}_p^{-T}$ gives the additive decomposition of the total stress into elastic, viscoelastic and equilibrium plastic parts in a similar way to that of total stored energy. Utilizing this, the dissipation inequality reduces to

$$-\frac{\partial \psi_v}{\partial \tilde{C}_{ev}}\frac{\partial \tilde{C}_{ev}}{\partial \tilde{F}_v} : \dot{\tilde{F}}_v - \frac{\partial \psi_p}{\partial \tilde{C}_{ep}}\frac{\partial \tilde{C}_{ep}}{\partial \tilde{F}_p} : \dot{\tilde{F}}_p \geq 0 \tag{2.20}$$

In which the first term is associated with viscoelastic dissipation and the second term associated with equilibrium hysteresis. This dissipation inequality should be satisfied for any arbitrary deformation processes. Following Lion (1997b), one way is to decouple the viscoelastic and plastic parts of the dissipation and make the each term positive so that the total dissipation inequality is satisfied.

Reducing the above equation to

$$\left\{-\tilde{\tau}_v : \frac{1}{2}\left(L_v \tilde{b}_{ev}\right)\cdot \tilde{b}_{ev}^{-1}\right\} + \left\{-\tilde{\tau}_p : \frac{1}{2}\left(L_v \tilde{b}_{eep}\right)\cdot \tilde{b}_{ep}^{-1}\right\} \geq 0 \tag{2.21}$$

Where,

$$\tilde{\tau}_v = 2\tilde{F}_{ev}\frac{\partial \psi_v}{\partial \tilde{C}_{ev}}\tilde{F}_{ev}^T \tag{2.22a}$$

$$\tilde{\tau}_p = 2\tilde{F}_{ep}\frac{\partial \psi_p}{\partial \tilde{C}_{ep}}\tilde{F}_{ep}^T \tag{2.22b}$$

To make Equation 2.21 positive definite and following Reese and Govindjee (1998a) for the viscoelastic case, the evolution equations of the following form are proposed.

$$-\frac{1}{2}\left(L_v \tilde{b}_{ev}\right)\cdot \tilde{b}_{ev}^{-1} = \tilde{\gamma}_v^{-1} : \tilde{\tau}_v \tag{2.23a}$$

$$-\frac{1}{2}\left(L_v\tilde{b}_{ep}\right)\cdot\tilde{b}_{ep}^{-1}=\dot{z}\,\tilde{\gamma}_p^{-1}:\tilde{\tau}_p \tag{2.23b}$$

Where, $\dot{z}$ is the kinematic arc length, which eliminates the rate dependency from plastic part of the evolution equation. These equations are also similar to that used by Lin and Schomburg (2003), though the Lin's equation can be reduced to the above equation, Equation 2.23b seems to be consistent with Equation 2.23a and assumes Valanis (1971) form. $\tilde{\gamma}_v$ and $\tilde{\gamma}_p$ are positive definite fourth order isotropic tensors and defined as

$$\tilde{\gamma}_v^{-1}=\frac{1}{2\eta_{Dv}}\left(\tilde{I}-\frac{1}{3}\tilde{I}\otimes\tilde{I}\right)+\frac{1}{9\eta_{Vv}}\tilde{I}\otimes\tilde{I} \tag{2.24a}$$

$$\tilde{\gamma}_p^{-1}=\frac{1}{2\eta_{Dp}}\left(\tilde{I}-\frac{1}{3}\tilde{I}\otimes\tilde{I}\right)+\frac{1}{9\eta_{Vp}}\tilde{I}\otimes\tilde{I} \tag{2.24b}$$

Equation 2.24a is the same as proposed by Reese and Govindjee (1998a) for viscoelastic dissipation. It is extended to represent equilibrium hysteresis as Equation 2.24b. η_{Dv} and η_{Vv} represent the deviatoric and volumetric viscosities respectively. η_{Dp} and η_{Vp} are the deviatoric and volumetric viscosities associated with plasticity. The first terms in each of the Equations 2.24a and 2.24b represent deviatoric part and the second term represents isochoric part. Substituting 2.24a and 2.24b in 2.23a and 2.23b

$$-\left(L_v\tilde{b}_{ev}\right)\cdot\tilde{b}_{ev}^{-1}=\frac{1}{\eta_{Dv}}dev\left(\tilde{\tau}_v\right)+\frac{2}{9\eta_{Vv}}\left(\tilde{\tau}_v:\tilde{I}\right) \tag{2.25a}$$

$$-\left(L_v\tilde{b}_{ep}\right)\cdot\tilde{b}_{ep}^{-1}=\dot{z}\left(\frac{1}{\eta_{Dp}}dev\left(\tilde{\tau}_p\right)+\frac{2}{9\eta_{Vp}}\left(\tilde{\tau}_p:\tilde{I}\right)\right) \tag{2.25b}$$

The evolution equations, called "flow rules", as an analogy with elastoplasticity, obtained in this work are the similar to that of equations derived by Lin and Schomburg (2003) but following a different procedure. In the current work Lie time derivatives along with push-

forward and pull-back operations to maintain the objectivity are used which has stronger thermodynamic base. On the other hand, Lin and Schomburg (2003) used corotational formulation for rate quantities involved in the dissipation inequality and arrived at the following equations.

$$\overset{\circ}{\tilde{\varepsilon}}^{\log} - \overset{\circ}{\tilde{\varepsilon}}_{ev} = \phi^{\gamma_{Vv}} \tilde{\gamma}_V^{-1} : \tilde{\tau}_v \tag{2.26a}$$

$$\overset{\circ}{\tilde{\varepsilon}}^{\log} - \overset{\circ}{\tilde{\varepsilon}}_{ep} = \dot{Z}\, \phi^{\gamma_p} \tilde{\gamma}_p^{-1} : \tilde{\tau}_p \tag{2.26b}$$

This completes the finite strain non-linear viscoelastic-plastic constitutive model. An efficient algorithm is to be employed in order to implement the model under numerical scheme.

2.3.1 Incompressibility

Often rubber is assumed to be incompressible in nature e.g. Ogden (1972). According to Holownia and James (1993), the effect of rate of deformation is very small on the dynamic bulk modulus. In the present context the material is assumed to be nearly incompressible. As proposed by Flory (1961) and successfully implemented by Simo (1988), Reese and Wriggers (1997) in the context of elastoplasticity, Lubliner (1985), Bonet (2001) for finite viscoelasticity, Weber and Anand (1990), Lion (1997b), for finite strain viscoplasticity, the following decomposition of the deformation gradient is used.

$$\tilde{F} = \hat{\tilde{F}}\bar{\tilde{F}} \tag{2.29}$$

Where,

$$\hat{\tilde{F}} = J^{\frac{1}{3}} \tilde{I} \tag{2.30}$$

$$\bar{\tilde{F}} = J^{-\frac{1}{3}}\tilde{F} \tag{2.31}$$

$\hat{F}$ is the volumetric part of the deformation gradient defined by equation 2.30 and $\bar{F}$ is the deviatoric part of the deformation gradient defined through equation 2.31. In the literature $\bar{F}$ is often referred to as modified deformation gradient. Also, in line with the above decomposition the following quantities are also defined.

$$\tilde{F}_{ev} = \hat{\tilde{F}}_{ev}\bar{\tilde{F}}_{ev} \tag{2.32}$$

$$\tilde{F}_{ep} = \hat{\tilde{F}}_{ep}\bar{\tilde{F}}_{ep} \tag{2.33}$$

Where,

$$\hat{\tilde{F}}_{ev} = J_{ev}^{\frac{1}{3}}\tilde{I}\ ,\ \bar{\tilde{F}}_{ev} = J_{ev}^{-\frac{1}{3}}\tilde{F}_{ev} \tag{2.34}$$

$$\hat{\tilde{F}}_{ep} = J_{ep}^{\frac{1}{3}}\tilde{I}\ ,\ \bar{\tilde{F}}_{ep} = J_{ep}^{-\frac{1}{3}}\tilde{F}_{ep} \tag{2.35}$$

Using the above decompositions the modified left Cauchy-Green deformation tensor for viscoelstic and plastic parts becomes,

$$\hat{\tilde{b}}_{ev} = \hat{\tilde{F}}_{ev}\hat{\tilde{F}}_{ev}^{T}\ ,\ \bar{\tilde{b}}_{ev} = \bar{\tilde{F}}_{ev}\bar{\tilde{F}}_{ev}^{T} \tag{2.36a}$$

$$\hat{\tilde{b}}_{ep} = \hat{\tilde{F}}_{ep}\hat{\tilde{F}}_{ep}^{T}\ ,\ \bar{\tilde{b}}_{ep} = \bar{\tilde{F}}_{ep}\bar{\tilde{F}}_{ep}^{T} \tag{2.36b}$$

To enable decoupled representation of the volume preserving and volume changing parts, the stored energy is also split into two parts (Holzapfel, 2000), as follows

$$\psi = \psi_{vol} + \psi_{iso} \tag{2.37}$$

It is worth noting here that the additive decomposition of the stored energy function is in addition to the decomposition of the stored energy into elastic, viscoelastic and plastic parts. Thus each function takes the form:

$$\psi_e = \left(\psi_{vol}\left(J\right)\right)_e + \left(\psi_{iso}\left(\bar{\bar{F}}\right)\right)_e \tag{2.38a}$$

$$\psi_{ev} = \left(\psi_{vol}\left(J_{ev}\right)\right)_{ev} + \left(\psi_{iso}\left(\bar{\bar{F}}_{ev}\right)\right)_{ev} \tag{2.38b}$$

$$\psi_{ep} = \left(\psi_{vol}\left(J_{ep}\right)\right)_{ep} + \left(\psi_{iso}\left(\bar{\bar{F}}_{ep}\right)\right)_{ep} \tag{2.38c}$$

2.4 ALGORITHEMIC IMPLEMENTATION

Exponential mapping along with operator split originally proposed by Weber and Anand (1990), Simo (1992), for elastic-plastic material is employed here to solve the viscoelastic and plastic evolution equations. It is a two stage algorithm, in the first stage approximate value is predicted and in the second stage predicted value is corrected. This prediction and correction continues in an iterative form till the equation is satisfied.

Let the material state at time t = n is completely known and the main objective of the algorithm is to evaluate the material state at time t = n+1. The main feature of the algorithm is that the inelastic part of the deformation gradient is assumed to be zero.. in the time increment n to n+1. The pictorial representation of the solution procedure is shown in Figure 2.3. The algorithm employed here is same as that of Reese and Govindjee (1998a), except that here one extra evolution equation for equilibrium hysteresis through endochronic theory of plasticity is added. Under this algorithm initially the increment in the deformation from t = n to t = n+1 is estimated as if it is entirely elastic, making the viscous velocity gradient and the plastic velocity gradient to be zero in the current increment. Thus

$$L_v \tilde{b}_{ev} = \dot{\tilde{b}}_{ev} \tag{2.39a}$$

$$L_v \tilde{b}_{ep} = \dot{\tilde{b}}_{ep} \tag{2.39b}$$

Initially a trial value of stress is calculated as if the whole of the strain is elastic. This trial values are corrected so that the evolution equations are satisfied.

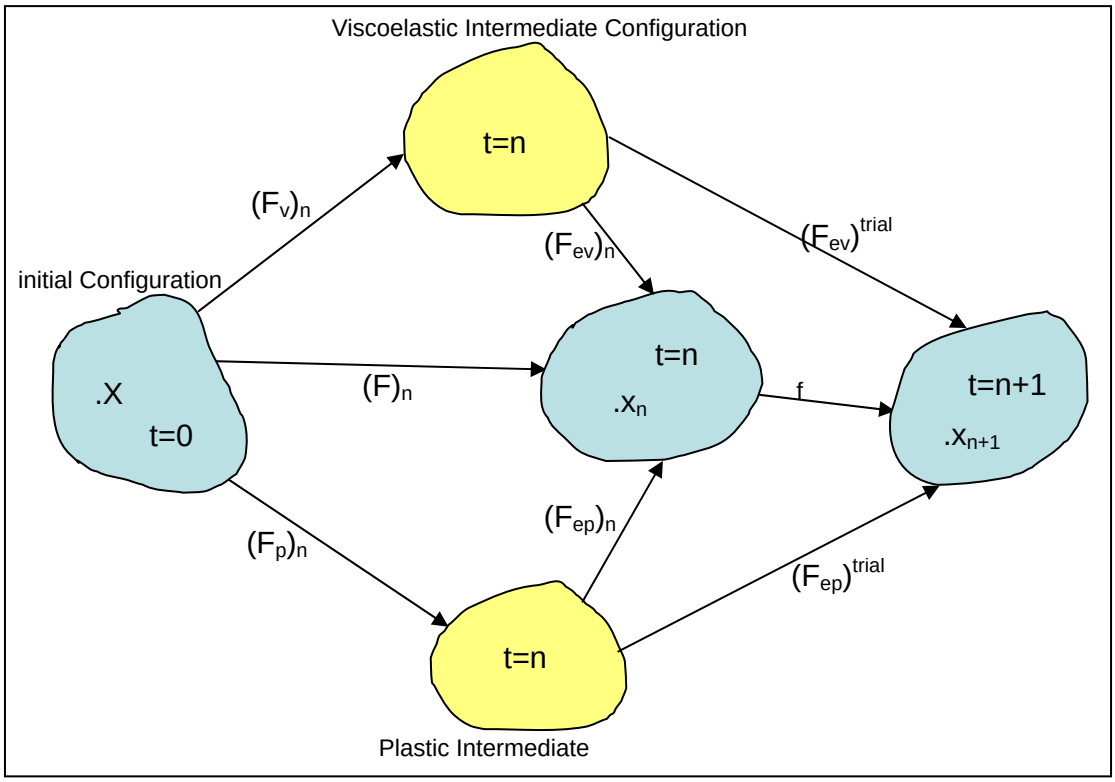

Fig. 2.3 Pictorial Representation of the Solution Procedure Using Exponential Mapping with Predictor-Corrector Method

Applying Equation 2.39a in 2.23a and 2.39b in 2.23b during time t = n to t = n+1

$$-\frac{1}{2}\dot{\tilde{b}}_{ev} \cdot \tilde{b}_{ev}^{-1} = \tilde{\gamma}_v^{-1} : \tilde{\tau}_v \tag{2.40a}$$

$$-\frac{1}{2}\dot{\tilde{b}}_{ep} \cdot \tilde{b}_{ep}^{-1} = \dot{z}\,\tilde{\gamma}_p^{-1} : \tilde{\tau}_p \tag{2.40b}$$

Further, applying exponential mapping to the Equations 2.40a and 2.40b

$$\tilde{b}_{ev} = \exp\left(-2 \int_{t_n}^{t_{n+1}} \tilde{\gamma}_v^{-1} : \tilde{\tau}_v \, dt \right) \left(\tilde{b}_{ev} \right)_{trial} \tag{2.41a}$$

$$\tilde{b}_{ep} = \exp\left(-2 \dot{z} \int_{t_n}^{t_{n+1}} \tilde{\gamma}_p^{-1} : \tilde{\tau}_p \, dt \right) \left(\tilde{b}_{ep} \right)_{trial} \tag{2.41b}$$

In Equations 2.41a and 2.41b $\left(\tilde{b}_{ev} \right)_{trial}$ and $\left(\tilde{b}_{ep} \right)_{trial}$ are given by

$$\left(\tilde{b}_{ev} \right)_{trial} = \tilde{F}_{n+1} \left(\tilde{C}_v^{-1} \right)_n \tilde{F}_{n+1}^T \tag{2.42a}$$

$$\left(\tilde{b}_{ep} \right)_{trial} = \tilde{F}_{n+1} \left(\tilde{C}_p^{-1} \right)_n \tilde{F}_{n+1}^T \tag{2.42b}$$

Integrating 2.41a and 2.41b

$$\left(\tilde{b}_{ev} \right)_{t_{n+1}} = \exp\left[-2 \left(t_{n+1} - t_n \right) \left(\gamma_v^{-1} : \tilde{\tau}_v \right) \right] \left(\tilde{b}_{ev} \right)_{trial} \tag{2.43a}$$

$$\left(\tilde{b}_{ep} \right)_{t_{n+1}} = \exp\left[-2 \dot{z} \left(t_{n+1} - t_n \right) \left(\gamma_p^{-1} : \tilde{\tau}_p \right) \right] \left(\tilde{b}_{ep} \right)_{trial} \tag{2.43b}$$

Substituting for $\tilde{\gamma}_v$ and $\tilde{\gamma}_p$ and writing $\Delta t = \left(t_{n+1} - t_n \right)$

$$\left(\tilde{b}_{ev} \right)_{t_{n+1}} = \exp\left[-\Delta t \left(\frac{1}{\eta_{Dv}} dev\left(\tilde{\tau}_v \right) + \frac{2}{9\eta_{Vv}} \tilde{\tau}_v : 1 \right) \right] \left(\tilde{b}_{ev} \right)_{trial} \tag{2.44a}$$

$$\left(\tilde{b}_{ep} \right)_{t_{n+1}} = \exp\left[-\dot{z} \Delta t \left(\frac{1}{\eta_{Dp}} dev\left(\tilde{\tau}_p \right) + \frac{2}{9\eta_{Vp}} \tilde{\tau}_p : 1 \right) \right] \left(\tilde{b}_{ep} \right)_{trial} \tag{2.44b}$$

The equations 2.44a and 2.44b are nonlinear in nature since the stresses $\tilde{\tau}_v$ and $\tilde{\tau}_p$ are functions of $\tilde{b}_{ev}$ and $\tilde{b}_{ep}$. It is easier to solve these equations in principal space, assuming isotropy, i.e., $\tilde{\tau}_v, \tilde{b}_{ev}$ and $\tilde{\tau}_p, \tilde{b}_{ep}$ are co-axial,

$$\left(\lambda_{ev}^2\right)_A = \exp\left[-\Delta t\left(\frac{1}{\eta_{Dv}} dev\left[\left(\tau_v\right)_A\right] + \frac{2}{9\eta_{Vv}}\left(\tau_v\right)_A : 1\right)\right]\left[\left(\lambda_{ev}^2\right)_A\right]_{trial} \tag{2.45a}$$

$$\left(\lambda_{ep}^2\right)_A = \exp\left[-\dot{z}\,\Delta t\left(\frac{1}{\eta_{Dp}} dev\left[\left(\tau_p\right)_A\right] + \frac{2}{9\eta_{Vp}}\left(\tau_p\right)_A : 1\right)\right]\left[\left(\lambda_{ep}^2\right)_A\right]_{trial} \tag{2.45b}$$

In the Equations 2.45a and 2.45b, A indicates the principal directions 1, 2, 3. $\left(\lambda_{ev}^2\right)_A$ and $\left(\lambda_{ep}^2\right)_A$ are the principal values of $\tilde{b}_{ev}$ and $\tilde{b}_{ep}$, $\left(\tau_v\right)_A$ and $\left(\tau_p\right)_A$ are the principal values of $\tilde{\tau}_v$ and $\tilde{\tau}_p$ respectively. Applying logarithm for equations 2.32a and 2.32b

$$\left(\varepsilon_{ev}\right)_A = -\Delta t\left(\frac{1}{\eta_{Dv}} dev\left[\left(\tau_v\right)_A\right] + \frac{2}{9\eta_{Vv}}\left(\tau_v\right)_A : 1\right) + \left[\left(\varepsilon_{ev}\right)_A\right]_{trial} \tag{2.46a}$$

$$\left(\varepsilon_{ep}\right)_A = -\dot{z}\,\Delta t\left(\frac{1}{\eta_{Dp}} dev\left[\left(\tau_p\right)_A\right] + \frac{2}{9\eta_{Vp}}\left(\tau_p\right)_A : 1\right) + \left[\left(\varepsilon_{ep}\right)_A\right]_{trial} \tag{2.46b}$$

Where, ε is the logarithmic stretch and is defined as $\varepsilon_A = \ln\left(\lambda_A\right)$

The Equations 2.46a and 2.46b are similar to that of Reese and Govindjee (1998a), the only difference is that here two evolution equations one for viscoelasticity and the other for equilibrium plasticity.

2.4.1 Local Newton-Raphson (N-R) iterations

Equations 2.33a and 2.33b are solved using N-R scheme since they are non-linear in nature. The step by step procedure for local N-R solution is given in Tables 2.1 and 2.2. Detailed expressions are given in Appendix A. Lin and Schomburg (2003) also obtained similar equations for representing viscoelasticity and elasto-plasticity in their finite elastic-viscoelstic-elastoplastic material law. However Lin and Schomburg (2006)

showed that the dissipation inequality with the objective rates is identical to the one with Lie time derivatives. They approximated objective rates to get the incremental solution, (refer to equation 38 to equation 44 in Lin and Schomburg, 2003). The two equations are reproduced below as Equation 2.47a and 2.47b for convenience. In other words, he has approximated an objective rate with a time rate. Though, it so happens that both the forms lead to the same equations at the end, Lie derivative usage followed here is consistent with the traditional approach in finite deformation elastoplasticity.

$$\overset{\circ}{\tilde{\varepsilon}}^{\log} - \overset{\circ}{\tilde{\varepsilon}}_{ev} = dt\phi^{\gamma_{Vv}} \tilde{\gamma}_V^{-1} : \tilde{\tau}_v \tag{2.47a}$$

$$\overset{\circ}{\tilde{\varepsilon}}^{\log} - \overset{\circ}{\tilde{\varepsilon}}_{ep} = dz\phi^{\gamma_p} \tilde{\gamma}_p^{-1} : \tilde{\tau}_p \tag{2.48b}$$

Table 2.1 Local N-R iteration loop for viscoelastic evolution equation

1. Let $\left(r_V\right)_A = \left(\varepsilon_{ev}\right)_A + \Delta t\left(\frac{1}{\eta_{Dv}} dev\left[\left(\tau_v\right)_A\right] + \frac{2}{9\eta_{Vv}}\left(\tau_v\right)_A : 1\right) - \left[\left(\varepsilon_{ev}\right)_A\right]_{trial}$ Let values of the variable to be calculated at K+1[th] increment form K[th] increment.

2.Linearizing $\left(r_V\right)_A$ w.r.t. $\left(\varepsilon_{ev}\right)_A$

$$\left[\left(r_V\right)_A\right]_{k+1} = \left[\left(r_V\right)_A\right]_k + \left(\frac{\partial\left[\left(r_V\right)_A\right]}{\partial\left[\left(\varepsilon_{ev}\right)_B\right]}\right)_k \left[\left(\Delta\varepsilon_{ev}\right)_B\right]_k = 0$$

3. Solve for $\left[\left(\Delta\varepsilon_{ev}\right)_B\right]$

4.Update $\left[\left(\varepsilon_{ev}\right)_A\right]_{k+1} = \left[\left(\varepsilon_{ev}\right)_A\right]_k + \left[\left(\Delta\varepsilon_{ev}\right)_A\right]_k$

5. Set k = k+1 and repeat till $\left\|\left(r_V\right)_A\right\| < tolerance$

Table 2.2 Local N-R iteration loop for equilibrium plastic evolution equation

1. Let $\left(r_P\right)_A = \left(\varepsilon_{ep}\right)_A + \dot{z}\,\Delta t\left(\frac{1}{\eta_{Dp}} dev\left[\left(\tau_p\right)_A\right] + \frac{2}{9\eta_{Vp}}\left(\tau_p\right)_A : 1\right) - \left[\left(\varepsilon_{ep}\right)_A\right]_{trial}$

Let values of the variable to be calculated at K+1th increment form Kth increment.

2.Linearizing $\left(r_P\right)_A$ w.r.t. $\left(\varepsilon_{ep}\right)_A$

$$\left[\left(r_P\right)_A\right]_{k+1} = \left[\left(r_P\right)_A\right]_k + \left(\frac{\partial\left[\left(r_P\right)_A\right]}{\partial\left[\left(\varepsilon_{ep}\right)_B\right]}\right)_k \left[\left(\Delta\varepsilon_{ep}\right)_B\right]_k = 0$$

3. Solve for $\left[\left(\Delta\varepsilon_{ep}\right)_B\right]$

4.Update $\left[\left(\varepsilon_{ep}\right)_A\right]_{k+1} = \left[\left(\varepsilon_{ep}\right)_A\right]_k + \left[\left(\Delta\varepsilon_{ep}\right)_A\right]_k$

5.Set k = k+1 and repeat till $\left\|\left(r_V\right)_A\right\| < tolerance$

2.5 CALCULATION OF DISSIPATION

Calculation of dissipation is important for various applications. As it has already been stated the two possible sources of dissipation are through viscosity and plasticity. Following Reese and Govindjee (1998b) the internal dissipation due to viscous effects can be written as

$$\mathrm{d}_v = -\tilde{\tau}_v : \frac{1}{2}\left(L_v \tilde{b}_{ev}\right)\cdot \tilde{b}_{ev}^{-1} \qquad (2.48a)$$

Similarly he plastic part of the dissipation can be estimated by using

$$\mathrm{d}_p = -\tilde{\tau}_p : \frac{1}{2}\left(L_v \tilde{b}_{eep}\right) \cdot \tilde{b}_{ep}^{-1} \tag{2.48b}$$

Reducing equations 2.48a and 2.48b using 2.46a and 2.46b

$$d_v = -\frac{\tilde{\tau}_v}{\Delta t}\left(\tilde{\varepsilon}_{ev} - \left(\tilde{\varepsilon}_{ev}\right)_{trial}\right) \tag{2.49a}$$

$$d_p = -\frac{\tilde{\tau}_p}{\dot{z}\,\Delta t}\left(\tilde{\varepsilon}_{ep} - \left(\tilde{\varepsilon}_{ep}\right)_{trial}\right) \tag{2.49b}$$

Adding 2.49a and 2.49b gives the total dissipation.

2.6 SUMMARY

A viscoelastic-plastic constitutive model has been developed. A plasticity model using endochronic theory of plasticity is used to represent equilibrium hysteresis. Two independent evolution equations are used, one representing viscoelasticity and the second for viscoplasticity. Product formula algorithm along with exponential mapping is used to integrate the evolution equation. The algorithm starts with the trial values for the viscoelastic and plastic internal variables and stresses and ends with two independent N-R iterative loops for correcting the trial values. The total dissipation can be calculated using Equations 2.49a and 2.49b.

CHAPTER 3

NUMERICAL IMPLEMENTATION

3.1 ABAQUS UMAT

The developed material model is implemented in the commercial finite element package ABAQUS (ABAQUS, 2005). ABAQUS offers three options for implementing user defined constitutive relations, which are known as UHYPER, UMAT and VUMAT. The subroutines can be coded using ANSI C or FORTRAN, depending on the availability of the compiler and proficiency of the user.

Of these three, VUMAT is the subroutine for the ABAQUS/Explicit and UHYPER and UMAT are the subroutines for ABAQUS/Standard which is an implicit code. Among UHYPER and UMAT, UHYPER is restricted to only a particular class of materials known as hyperelastic materials, whereas UMAT has no such restriction and can be used for any constitutive relation that includes mechanical behavior. It is easier to implement UHYPER, since it only requires the derivatives of the strain energy density function of the hyperelastic material defined with respect to strain invariants.

UMAT is provided with a larger range of inputs and can be used to update the solution dependent variables, which is required for the developed viscoelastic-plastic constitutive model. Since the material stiffness matrix needs to be updated by the user, it is difficult to

achieve convergence unless the matrix defined is exact or consistent. The developed viscoelastic-plastic constitutive model is implemented through UMAT.

The UMAT subroutine will be called at each integration point of an element for which user material is specified. In UMAT the Cauchy stress and the material Jacobian matrix need to be calculated and updated to ABAQUS/Standard.

3.2 MATERIAL JACOBIAN MATRIX

According to ABAQUS/Standard analysis user's manual (ABAQUS, 2005), the material Jacobian matrix is given by

$$C_{IJKL} = \frac{1}{\mathrm{J}} \frac{\partial \Delta \tau_{IJ}}{\partial \Delta \varepsilon_{KL}} \tag{3.1}$$

where,

C_{IJKL} is the exact consistent Jacobian matrix

J is the determinant of deformation gradient

τ_{IJ} is the Kirchhoff stress

ε_{KL} is the strain

Equation 3.1 can be viewed as the tangent modulus of the Jaumann rate of Kirchhoff stress. In standard literature it is represented as $\tilde{C}^{\tau J}$. Alternatively this expression can also be given by Belytschko *et al.* (2000).

$$\mathrm{J}^{-1} C^{\tau J}_{IJKL} = C^{\sigma \mathrm{T}}_{IJKL} + C'_{IJKL} \tag{3.2}$$

where,

$C^{\sigma \mathrm{T}}_{IJKL}$ is the tangent modulus for the Truesdell rate of Cauchy stress.

$$C'_{IJKL} = \frac{1}{2}\left(\delta_{IK}\sigma_{JL} + \delta_{IL}\sigma_{JK} + \delta_{JK}\sigma_{IL} + \delta_{JL}\sigma_{IK} \right) \tag{3.3}$$

For a hyperelastic constitutive relation the Truesdell rate of Cauchy stress is given by

$$C^{\sigma \mathrm{T}}_{IJKL} = J^{-1} C^{\tau}_{IJKL} \tag{3.4}$$

Where,

J is the determinant of the deformation gradient

C^{τ}_{IJKL} is the spatial tangent moduli

The spatial tangent moduli is calculated using

$$C^{\tau}_{IJKL} = 4 F_{IM}\ F_{JN}\ F_{KP}\ F_{LQ} \frac{\partial^2 \psi}{\partial C_{MN} \partial C_{PQ}} \tag{3.5}$$

As can be observed from the above equations the material Jacobian matrix is a 4th order tensor involving 81 elements. It can also be noted that $C^{\sigma \mathrm{T}}_{IJKL}$ has major symmetry and C'_{IJKL} is also a symmetric tensor which in turn results in symmetry of material Jacobian matrix. This symmetric property reduces the number of independent components to 36. These 36 components can be represented by a 6 x 6 matrix, which is known as material constitutive matrix in typical finite element terminology. In UMAT, ABAQUS requires this material constitutive matrix to be updated from the user code.

All the stored energy functions are assumed to be of Yeoh form (Yeoh, 1993). All simulations for monotonic tension use with displacement control except for creep

simulation in which load control is used. 8 node brick element is used with three degrees of freedom (dof) on each node.

3.3 CALCULATION OF EIGEN VALUES AND EIGEN VECTORS

To make the material model numerically efficient all the equations are transformed into principal space. Under the usual conditions of isotropy the program needs 6 independent components to be calculated from constitutive relations for the evaluation of stress tensor. The same reduces to 3 components if equations are transformed to principal space. In the proposed constitutive model at many places matrices are to be multiplied. Transformation of all these matrices to principal space reduces the enormous amount of computational time. Also, in the present case there are many matrices to be updated as solution dependent variables transforming all these into principal space will reduce the amount of data to be stored. This is very useful when the UMAT is applied to big problems such as rolling resistance prediction of an automobile tire. Also transformation to the principal space offers lesser number of variables and hence lesser ambiguity.

Because of the above advantages, the constitutive model is transformed to principal space initially and in the last stages the stress components and the material Jacobian matrix are rotated back to the original Cartesian frame using the Eigen vectors and then updated to ABAQUS. To evaluate the Eigen values and Eigen vectors of the various matrices involved Jacobi iteration method is used. The main advantage of the Jacobi iteration method is its reliability, as it guarantees solution for all real symmetric matrices. Also for

matrix sizes below 10 x 10 this method is competitive with more sophisticated methods. All the matrices for which Eigen values are to be found out in the present case are of 3 x 3 order. Under this method the matrix under consideration is multiplied with a transformation matrix which converts the chosen set of off-diagonal element to zero, this transformations are continued till all the off-diagonal elements are with in the predetermined tolerance. The transformation matrix is updated at each iteration and the final matrix represents the eigen vectors as its columns.

3.4 ALGORITHM

UMAT Algorithm for developed viscoelastic-plastic constitutive model

1. Get $\tilde{F}_n, \tilde{F}_{n-1}$, from ABAQUS input arguments and $\left(\tilde{C}_v^{-1}\right)_{n-1}, \left(\tilde{C}_p^{-1}\right)_{n-1}$ from the state variables.
2. Calculate $J, \tilde{b}_n, \left(\tilde{b}_{ev}\right)_n^{trial}, \left(\tilde{b}_{ep}\right)_n^{trial}$

   $$J = \det(\tilde{F})$$

   $$\tilde{b}_n = \tilde{F}_n \tilde{F}_n^T$$

   $$\left(\tilde{b}_{ev}\right)_n^{trial} = \tilde{F}_n \left(\tilde{C}_v^{-1}\right)_{n-1} \tilde{F}_n^{-1}$$

   $$\left(\tilde{b}_{ep}\right)_n^{trial} = \tilde{F}_n \left(\tilde{C}_p^{-1}\right)_{n-1} \tilde{F}_n^{-1}$$

3. Calculate $\bar{\tilde{b}}_n, \left(\bar{\tilde{b}}_{ev}\right)_n^{trial}, \left(\bar{\tilde{b}}_{ep}\right)_n^{trial}$

$$\bar{\tilde{b}}_n = J^{-\frac{2}{3}} \tilde{b}_n$$

$$\left(\bar{\tilde{b}}_{ev}\right)_n^{trial} = J_{ev}^{-\frac{2}{3}} \left(\tilde{b}_{ev}\right)_n^{trial}$$

$$\left(\bar{\tilde{b}}_{ep}\right)_n^{trial} = J_{ep}^{-\frac{2}{3}} \left(\tilde{b}_{ep}\right)_n^{trial}$$

4. Transform $\bar{\tilde{b}}_n, \left(\bar{\tilde{b}}_{ev}\right)_n^{trial}, \left(\bar{\tilde{b}}_{ep}\right)_n^{trial}$ to principal space to obtain principal values and principal directions.

5. Calculate $\tilde{\varepsilon}_n, \left(\tilde{\varepsilon}_{ev}\right)_n^{trial}, \left(\tilde{\varepsilon}_{ep}\right)_n^{trial}$

$$\tilde{\varepsilon}_n = \ln\left(\tilde{\lambda}_n\right)$$

$$\left(\tilde{\varepsilon}_{ev}\right)_n^{trial} = \ln\left(\left(\tilde{\lambda}_{ev}\right)_n^{trial}\right)$$

$$\left(\tilde{\varepsilon}_{ep}\right)_n^{trial} = \ln\left(\left(\tilde{\lambda}_{ep}\right)_n^{trial}\right)$$

6. Calculate $\tilde{\tau}_n, \left(\tilde{\tau}_{ev}\right)_n^{trial}, \left(\tilde{\tau}_{ep}\right)_n^{trial}$

$$\tilde{\tau}_n = \frac{\partial \psi_e}{\partial \tilde{\varepsilon}_n}$$

$$\left(\tilde{\tau}_{ev}\right)_n^{trial} = \frac{\partial \psi_v}{\partial \left(\tilde{\varepsilon}_{ev}\right)_n^{trial}}$$

$$\left(\tilde{\tau}_{ep}\right)_n^{trial} = \frac{\partial \psi_v}{\partial \left(\tilde{\varepsilon}_{ep}\right)_n^{trial}}$$

7. Calculate the final values of $\left(\tilde{\tau}_{ev}\right)_n, \left(\tilde{\tau}_{ep}\right)_n, \left(\tilde{\varepsilon}_{ev}\right)_n$ and $\left(\tilde{\varepsilon}_{ep}\right)_n$ using two independent local N-R iterations as described in Tables 2.1 and 2.2.
8. Calculate the material Jacobian matrix as described in section 3.2
9. Calculate $\tilde{\sigma}_n, \left(\tilde{\sigma}_{ev}\right)_n$, and $\left(\tilde{\sigma}_{ep}\right)_n$

$$\tilde{\sigma}_n = \frac{1}{J}\tau_n$$

$$\left(\tilde{\sigma}_{ev}\right)_n = \frac{1}{J_{ev}}\left(\tilde{\tau}_{ev}\right)_n$$

$$\left(\tilde{\sigma}_{ep}\right)_n = \frac{1}{J_{ep}}\left(\tilde{\tau}_{ep}\right)_n$$

10. Update state variables for $\left(\tilde{C}_v^{-1}\right)_n, \left(\tilde{C}_p^{-1}\right)_n$
11. Calculate viscoelastic and plastic dissipation using

$$d_v = -\frac{\tilde{\tau}_v}{\Delta t}\left(\tilde{\varepsilon}_{ev} - \left(\tilde{\varepsilon}_{ev}\right)_{trial}\right)$$

$$d_p = -\dot{z}\frac{\tilde{\tau}_p}{\Delta t}\left(\tilde{\varepsilon}_{ep} - \left(\tilde{\varepsilon}_{ep}\right)_{trial}\right)$$

12. Update stress tensor and material Jacobian for ABAQUS.

3.5 SIMULATION USING ABAQUS/Standard

All the stored energy functions of springs i.e. elastic, viscoelastic and plastic contributions are assumed to be of Yeoh form, as specified below.

$$\psi_e = (C_{10})_e(\bar{I}_1 - 3) + (C_{20})_e(\bar{I}_1 - 3)^2 + (C_{30})_e(\bar{I}_1 - 3)^3 + \frac{1}{D_e}(J_e - 1)^2 \quad (3.6a)$$

$$\psi_v = (C_{10})_v(\bar{I}_1 - 3) + (C_{20})_v(\bar{I}_1 - 3)^2 + (C_{30})_v(\bar{I}_1 - 3)^3 + \frac{1}{D_v}(J_{ev} - 1)^2 \quad (3.6b)$$

$$\psi_p = (C_{10})_p(\bar{I}_1 - 3) + (C_{20})_p(\bar{I}_1 - 3)^2 + (C_{30})_p(\bar{I}_1 - 3)^3 + \frac{1}{D_p}(J_{ep} - 1)^2 \quad (3.6c)$$

All the finite element simulations for monotonic tension were run on a single element of unit size as shown in Figure 3.1. C3D8 is the element type which is a linear brick element with three dof on each node. Displacement control is used for all simulations except in creep simulation.

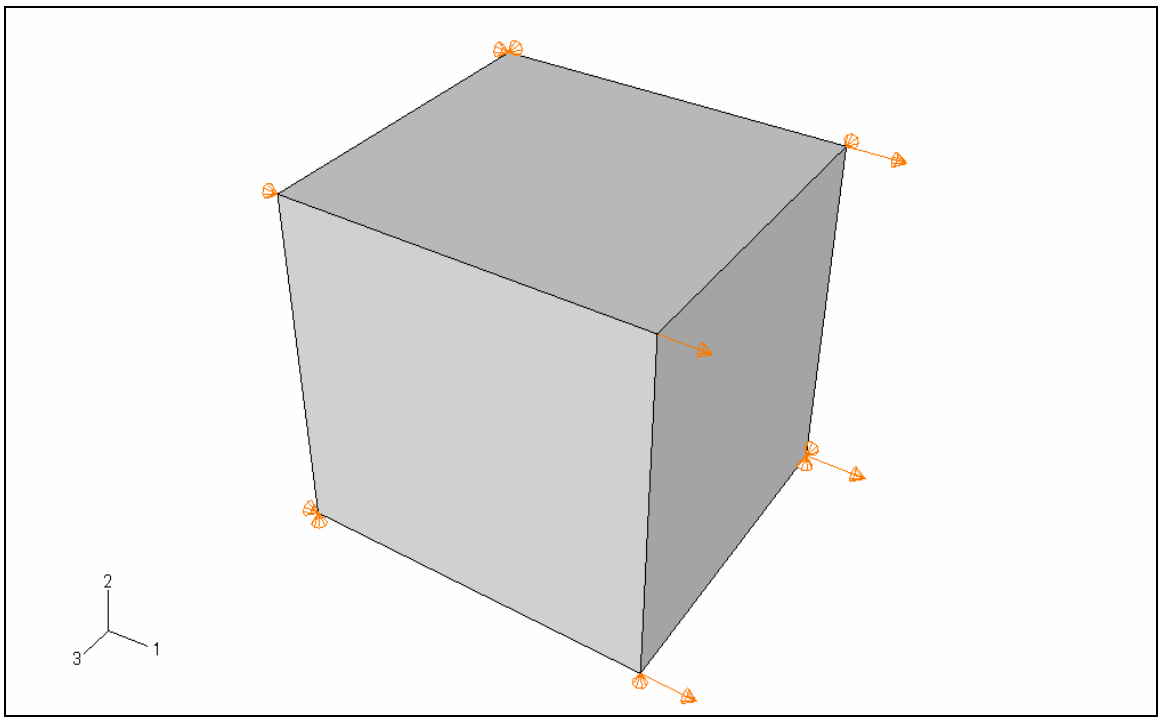

Fig. 3.1 Monotonic Tension Test Single Element Showing Boundary Conditions

3.6 SUMMARY

ABAQUS/Standard UMAT is used to implement the developed viscoelastic-plastic constitutive model. UAMT is a powerful tool and it needs stress and material Jacobian to be updated from the used code written in ANSI C or FORTRAN. An expression for the material model is derived. A procedure for deriving Eigen values and Eigen vectors is adopted from the Jacobi iteration method. The total algorithm for UMAT is described as a step by step procedure.

CHAPTER 4

RESULTS AND DISCUSSION

4.1 UNI-AXIAL SIMULATIONS WITH PROPOSED CONSTITUTIVE MODEL

In this section the developed constitute model is studied for its intended deformation behavior i.e viscoelastic and equilibrium hysteresis. The constitutive model is studied by conducting numerical experiments to understand its sensitivity to the material parameters involved. Figure 4.1 shows the effect of the rate of loading on the stress strain curve.

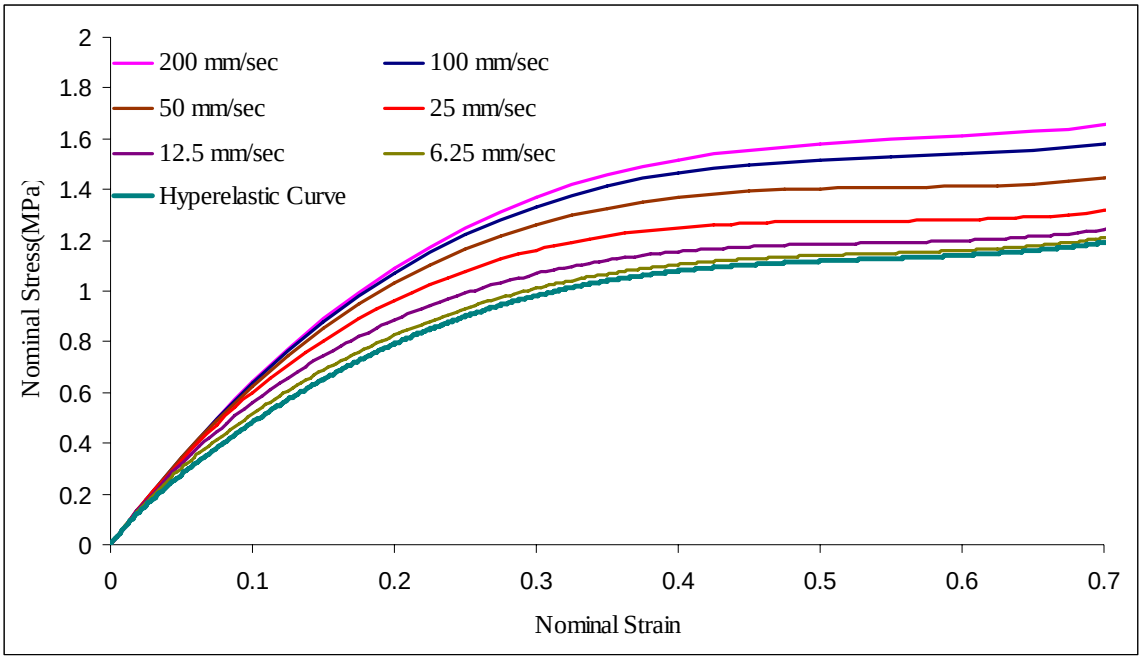

Fig. 4.1 Variation of Nominal Stress with Rate of Loading

The rate of loading is varied from 6.25 mm/sec to 200 mm/sec. It can be observed from figure that there is a significant effect of the rate of loading on the stress strain curve.

The curves approach the hyperelastic curve as the rate of loading is reduced. The hyperelastic curve is obtained by fitting Yeoh constants for the equlibium uni-axial tension experimental curve given by Haupt and Sedlan (2000). The viscoelastic and plastic constants are arbitrarily chosen. The material constants used for this study are listed in Table 4.1 as SET 2 constants

Table4.1 Constants for viscoelastic-plastic material model

Description	SET1 Constants	SET 2 Constants	SET 3 Constants	SET4 Constatnts
C_{10el} (MPa)	0.4195	0.8390	0.8390	0.2098
C_{20el} (MPa)	-0.1816	-0.3632	-0.3632	-0.0908
C_{30el} (MPa)	0.0599	0.1198	0.1198	0.0299
C_{10ev} (MPa)	0.4195	0.2098	0.2797	0.8390
C_{20ev} (MPa)	-0.1816	-0.0908	-0.1211	-0.3632
C_{30ev} (MPa)	0.0599	0.0299	0.03994	0.1198
η_{Dv} (MPa/sec)	1.0	1.0	1.0	1.0
C_{10ep} (MPa)	0.4195	0.2098	0.1398	0.2098
C_{20ep} (MPa)	-0.1816	-0.0908	-0.0605	-0.0908
$C30_{ep}$ (MPa)	0.0599	0.0299	0.0199	0.0299
η_{Dp} (MPa/sec)	5.0	5.0	5.0	5.0

Figures 4.2 and 4.3 shows the strain input and stress response for the creep loading, in the simulation load control is used with 0.75 N load applied in 0.25 sec and then the load is kept constant for 5 sec. From figure it can be observed that the strain increases even if the load is kept constant after 0.25 sec. This is due to the viscous nature of the constitutive model.

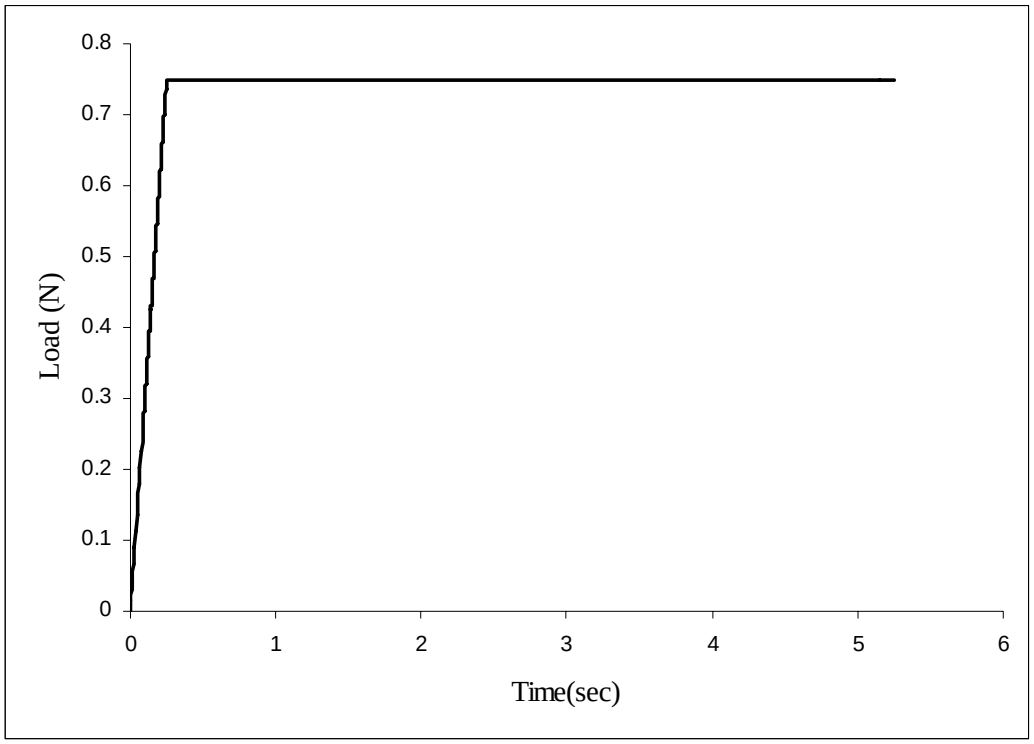

Fig 4.2 Input Load for Creep Test

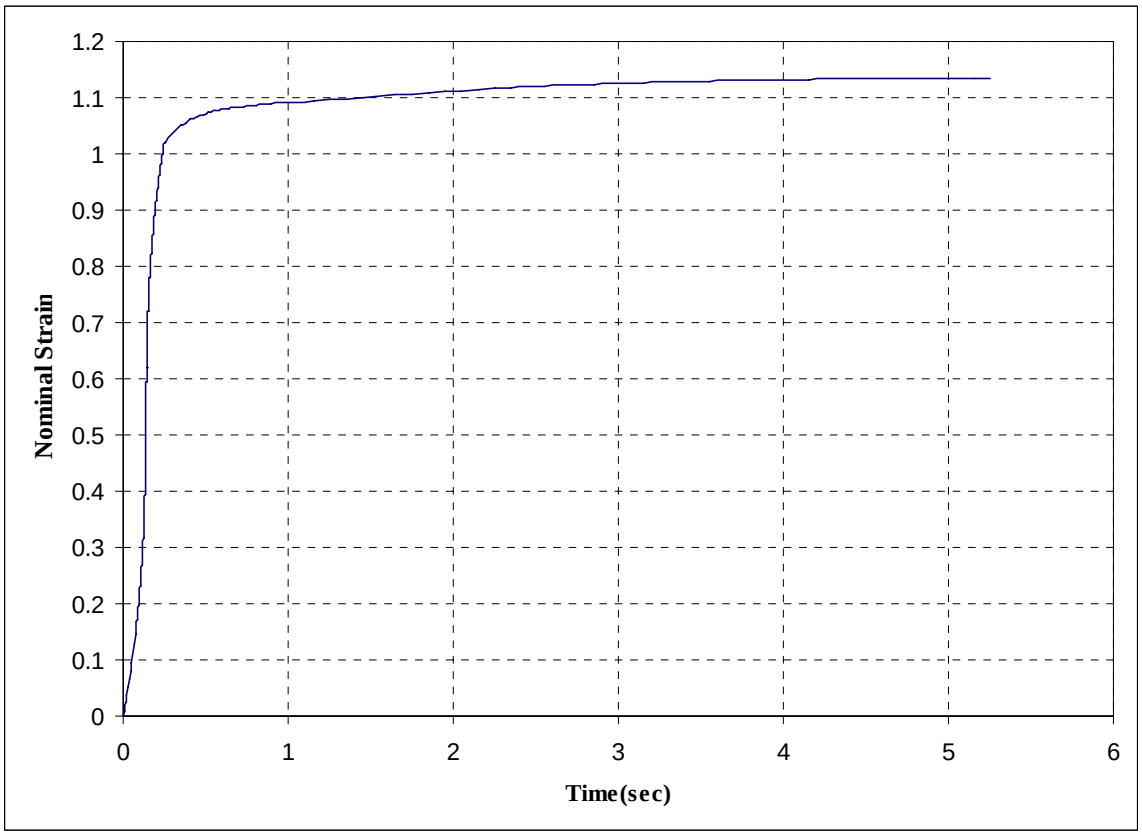

Fig. 4.3 Increase of Strain at Constant Load in Creep Test

In order to observe the presence of the equilibrium hysteresis, a uni-axial tension simulation is run at quasi static loading conditions. The resulting nominal stress vs. nominal strain graph is shown in Figure 4.4. It can be observed from the figure dissipation is present even at quasi static loading conditions. This dissipation is due to equilibrium hysteresis present in the model through plasticity.

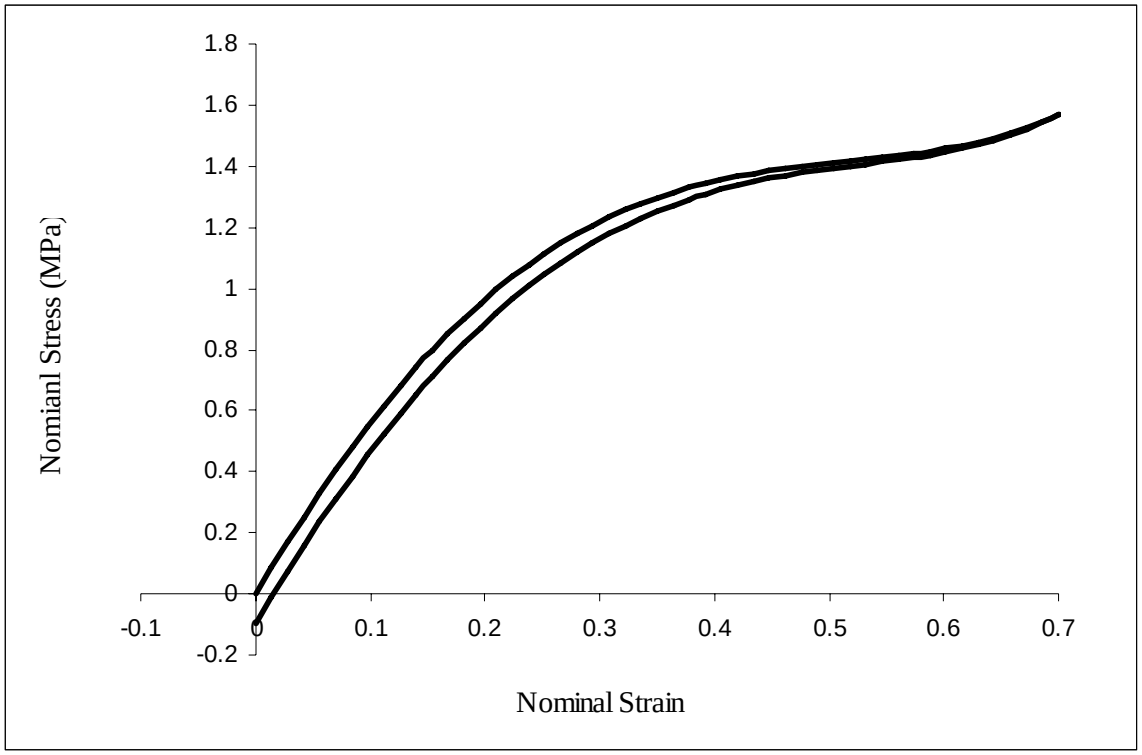

Fig. 4.4 Presence of Equilibrium Hysteresis at Quasi Static Loading

To observe the effect of elastic spring constants compared to viscoelastic and plastic constants, a uni-axial tension test is simulated with three different material constants as shown in Table 4.1. Figure 4.5 shows the comparison of the nominal stress vs. nominal strain graph for three different constants SET 1, SET 2 and SET 3. The Yeoh constants for elastic part of the stored energy function are the same in SET 2 and SET 3. From figure it can be observed that the change in nominal stress-nominal strain curve for SET 2 and SET 3 is low compared to that of SET 1 constants, this is because the elastic Yeoh stored energy constants for SET 1 differ by one order of magnitude compared to SET 2 and SET 3 constants. Whereas among SET 2 and SET 3 the viscoelastic and plastic part of stored energy function are changed significantly and the elastic part is not changed.

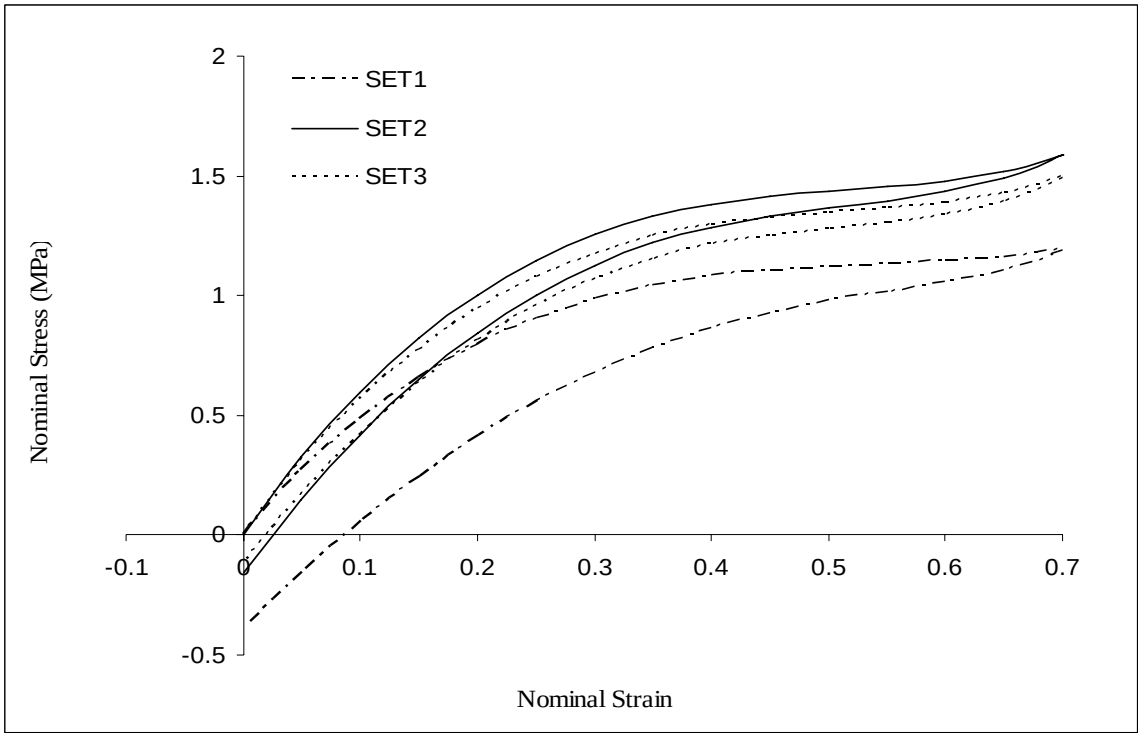

Fig 4.5 Effect of Elastic Constants Compared to Viscoelstic and Plastic Spring Constants

In the table for SET 4 constants the viscoelastic and elastic spring constants of SET 1 constants are interchanged to observe the effect of springs. Figure 4.6 shows the effect of interchanging viscoelastic and elastic spring constants. From the figure it can be observed that effect of interchanging the spring constants is not linear, in other words if it had been the linear relation among all the spring constants, both constants give same curve.

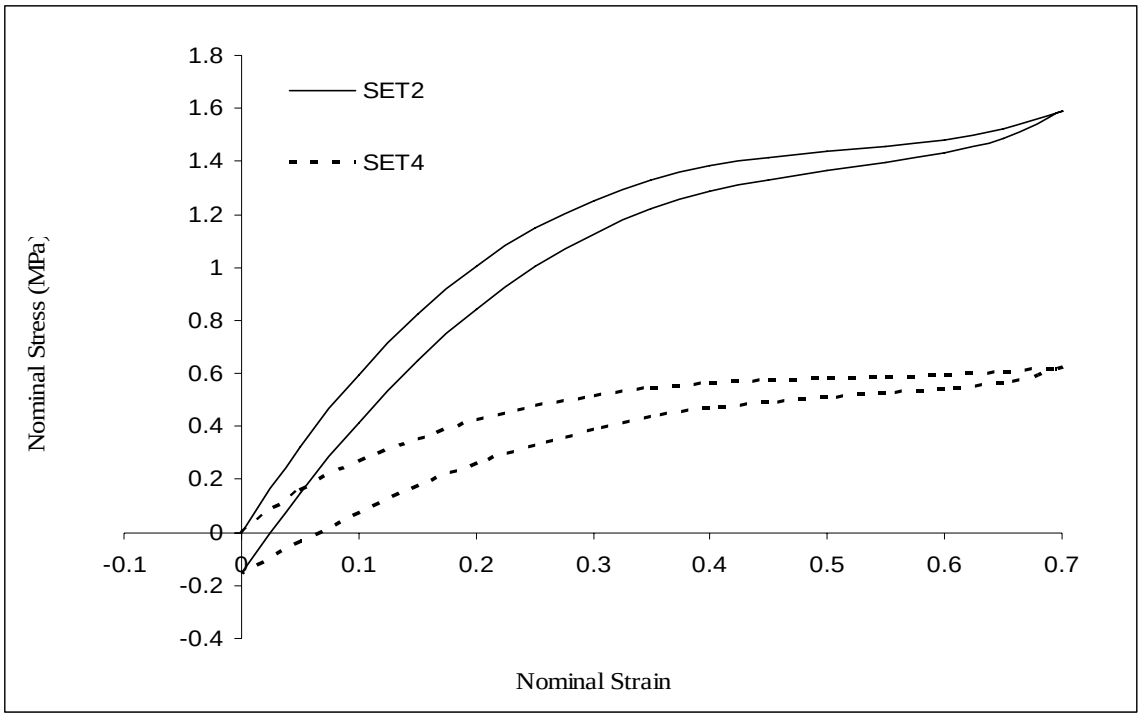

Fig 4.6 Effect of Interchanging the Spring Constants

4.1.1 Effect of elastic spring constants

In this section the effect of elastic spring constants alone is studied. Table 4.2 shows two sets of constants namely SET 1 and SET 5. Only elastic spring constants are varied and other constants are not changed. Figure 4.7 shows the effect of changing the elastic spring constants. It can be observed from the figure that even though the shape of the curve is changed significantly the amount of dissipation is not changed. This is because the dissipation is only a function of viscoelastic and plastic parameters.

Table 4.2 Constants used for studying the effect of elastic spring constants

Description	SET 1 Constants	SET5 Constants
C_{10el} (MPa)	0.4195	0.8390
C_{20el} (MPa)	-0.1816	-0.3632
C_{30el} (MPa)	0.0599	0.1198
C_{10ev} (MPa)	0.4195	0.4195
C_{20ev} (MPa)	-0.1816	-0.1816
C_{30ev} (MPa)	0.0599	0.0599
η_{Dv} (MPa /sec)	1.0	1.0
C_{10ep} (MPa)	0.4195	0.4195
C_{20ep} (MPa)	-0.1816	-0.1816
$C30_{ep}$ (MPa)	0.0599	0.0599
η_{Dp} (MPa/sec)	5.0	5.0

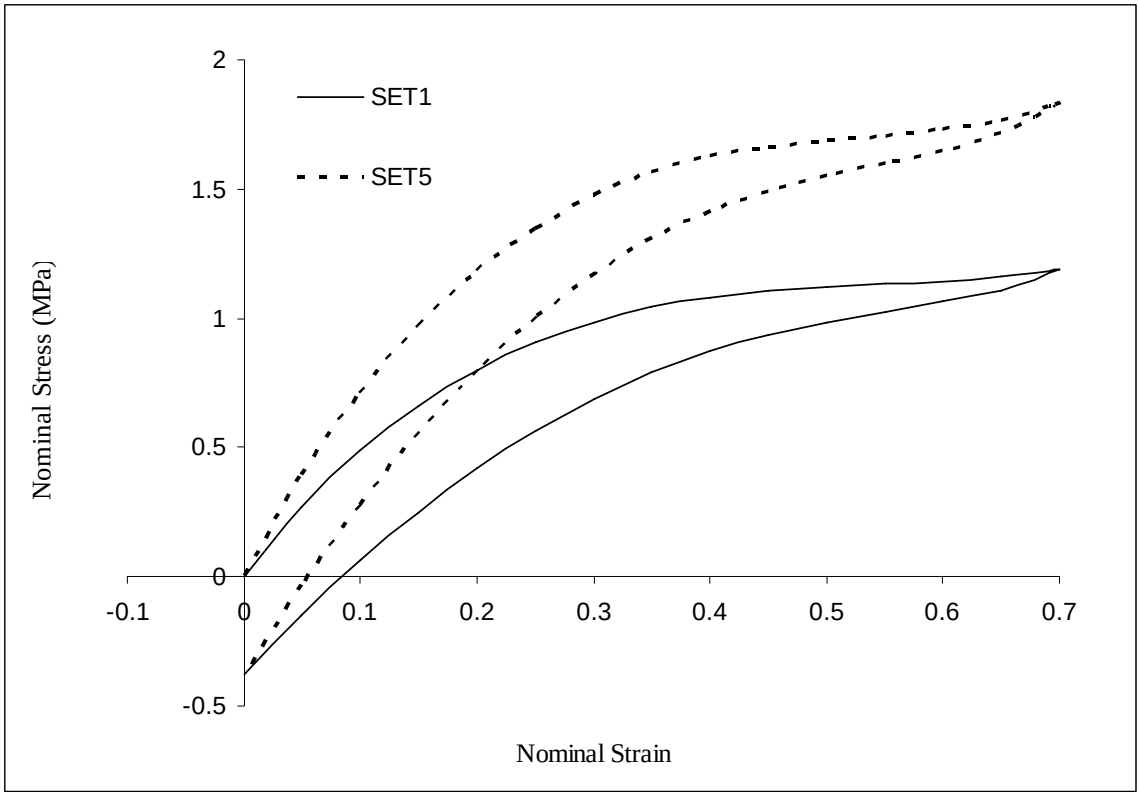

Fig. 4.7 Effect of Elastic Spring Constants

4.1.2 Effect of viscoelastic spring constants

To understand the effect of viscoelastic spring constants, they are varied as listed in Table 4.3. Only viscoelastic spring constants are varied among SET 6 and SET 7 constants. Figure 4.8 shows the effect of changing the viscoelastic spring constants. From the figure it can be observed that SET 6 constants show more dissipation compared to SET 7 constants. From the figure it is also evident that besides changing the amount of dissipation, the viscoelastic spring constants are also affecting the shape of the curve. This is because this change has a direct bearing on the strain in the dashpot and hence the change in the dissipated energy.

Table 4.3 Constants used for studying the effect of viscoelastic spring constants

Description	SET 6 Constants	SET7 Constants
C_{10el} (MPa)	0.4195	0.4195
C_{20el} (MPa)	-0.1816	-0.1816
C_{30el} (MPa)	0.0599	0.0599
C_{10ev} (MPa)	0.1398	0.4195
C_{20ev} (MPa)	-0.0605	-0.1816
C_{30ev} (MPa)	0.0199	0.0599
η_{Dv} (MPa /sec)	10	10
C_{10ep} (MPa)	0.4195	0.4195
C_{20ep} (MPa)	-0.1816	-0.1816
$C30_{ep}$ (MPa)	0.0599	0.0599
η_{Dp} (MPa/sec)	5.0	5.0

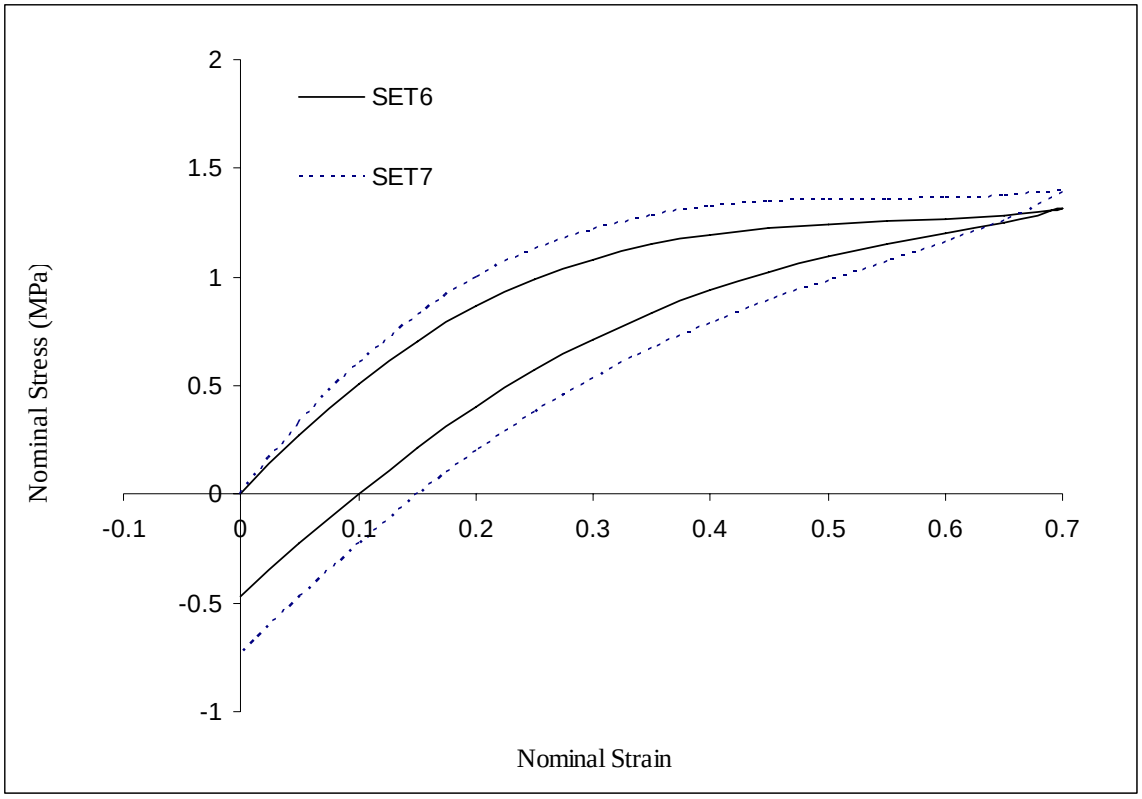

Fig. 4.8 Effect of Viscous Spring Constants on Monotonic Tension

4.1.3 Effect of plastic spring constants

To observe the effect of plastic spring constants the simulation is run with two different constants as listed in Table 4.4. Only plastic spring constants are varied among SET 1 and SET 8 constants. Figure 4.9 shows the stress strain curves for the constants given in Table 4.4. It can be observed from the figure that amount of dissipation is more for SET 1 constants. It can also be observed from the figure that the plastic spring constants also affect the shape as well as total dissipation.

Table 4.4 Constants used for studying the effect of plastic spring constants

Description	SET 1 Constants	SET 8 Constants
C_{10el} (MPa)	0.4195	0.4195
C_{20el} (MPa)	-0.1816	-0.1816
C_{30el} (MPa)	0.0599	0.0599
C_{10ev} (MPa)	0.4195	0.2797
C_{20ev} (MPa)	-0.1816	-0.1211
C_{30ev} (MPa)	0.0599	0.03994
η_{Dv} (MPa /sec)	1.0	1.0
C_{10ep} (MPa)	0.4195	0.1398
C_{20ep} (MPa)	-0.1816	-0.0605
$C30_{ep}$ (MPa)	0.0599	0.0199
η_{Dp} (MPa/sec)	5.0	5.0

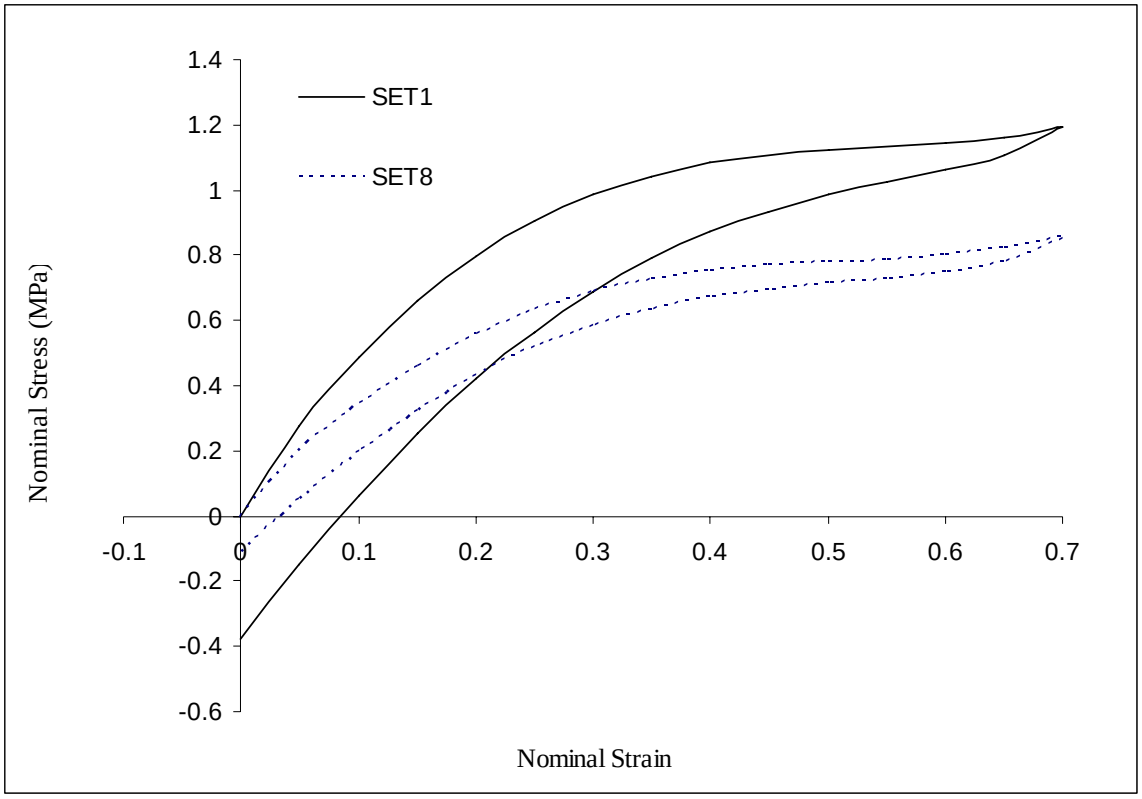

Fig. 4.9 Effect of Plastic Spring Constants on Equilibrium Hysteresis

4.1.4 Effect of viscoelastic dissipation parameter η_{Dv}

In this section the effect of viscoelastic dissipation parameter η_{Dv} is studied. Table 4.5 lists two sets of constants in which only η_{Dv} is changed from 1.0 MPa/sec to 10 MPa/sec. Figure 4.10 shows the nominal stress vs. nominal strain curves for the constants listed in Table 4.5. From the figure it can be observed that the dissipation is more with increase in η_{Dv} value. The shape of the curve is also affected with change in η_{Dv} value.

Table 4.5 Constants used for studying the effect of viscoelastic dissipation parameter η_{Dv}

Description	SET 1 Constants	SET 7 Constants
C_{10el} (MPa)	0.4195	0.4195
C_{20el} (MPa)	-0.1816	-0.1816
C_{30el} (MPa)	0.0599	0.0599
C_{10ev} (MPa)	0.4195	0.4195
C_{20ev} (MPa)	-0.1816	-0.1816
C_{30ev} (MPa)	0.0599	0.0599
η_{Dv} (MPa /sec)	1.0	10
C_{10ep} (MPa)	0.4195	0.4195
C_{20ep} (MPa)	-0.1816	-0.1816
$C30_{ep}$ (MPa)	0.0599	0.0599
η_{Dp} (MPa/sec)	5.0	5.0

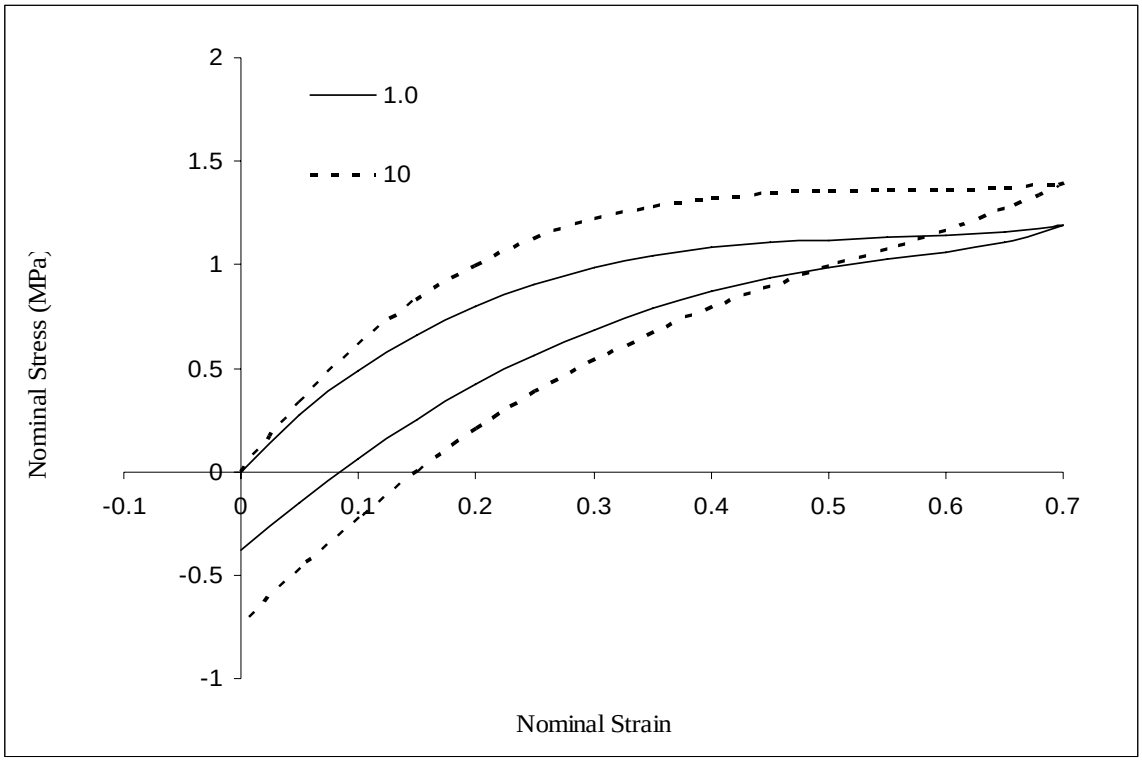

Fig. 4.10 Effect of Viscous Damping Constant η_{Dv} on Monotonic Tension

Figure 4.11 shows the effect of η_{Dv} on relaxation curve. The total strain input is given in 35 sec and then the material is allowed to relax under no load conditions for about 500 sec. From the figure it can be observed that the amount of relaxation is more with the increased η_{Dv} value. It can also be observed that the curves converge to the same value of stress since equilibrium response which is defined through elastic and plastic parameters are not varied.

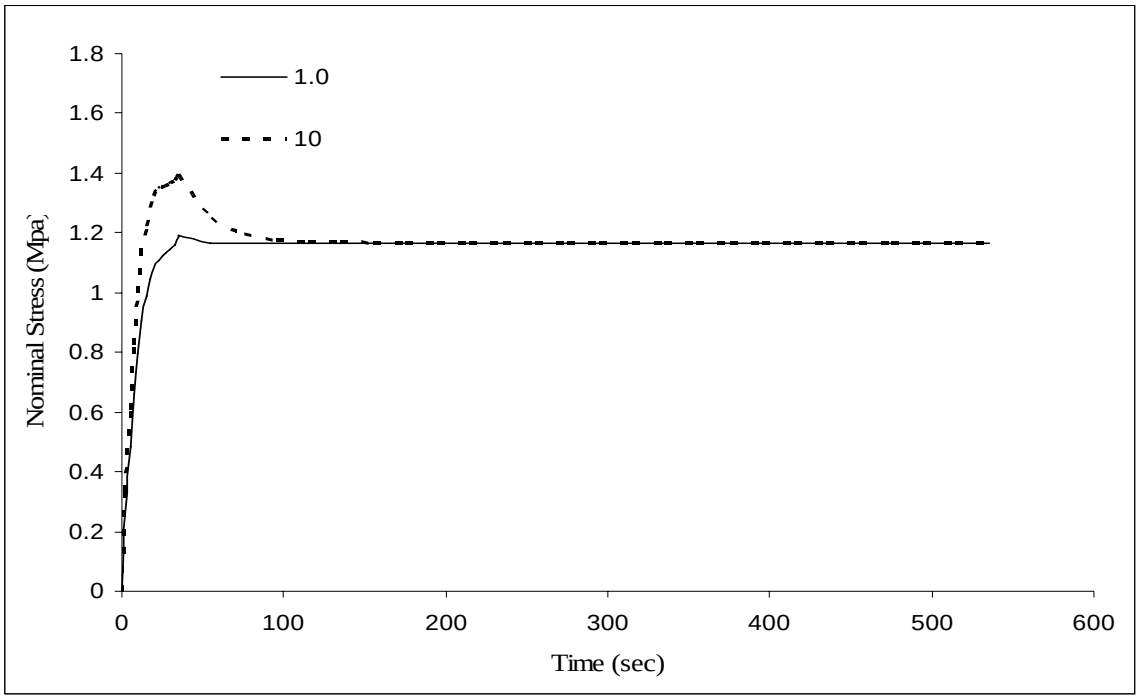

Fig. 4.11 Effect of Viscous Damping Constant η_{Dv} on relaxation

4.1.5 Effect of plastic dissipation parameter η_{Dp}

Finally, to study the effect of η_{Dp} two sets of constants in which its value is changed from 0.5 MPa/sec to 5.0 MPa/sec. Table 4.6 shows the constants used for this study. Figure 4.12 shows the effect of increasing the plastic dissipation parameter. It can be observed from the figure that the amount of dissipation increases with decrease in the value of η_{Dp}. The shape of curve is also gets affected as a result of change in η_{Dp} values.

Table 4.6 Constants used for studying the effect of plastic dissipation parameter η_{Dp}

Description	SET 1 Constants	SET 9 Constants
C_{10el} (MPa)	0.4195	0.4195
C_{20el} (MPa)	-0.1816	-0.1816
C_{30el} (MPa)	0.0599	0.0599
C_{10ev} (MPa)	0.4195	0.4195
C_{20ev} (MPa)	-0.1816	-0.1816
C_{30ev} (MPa)	0.0599	0.0599
η_{Dv} (MPa /sec)	1.0	1.0
C_{10ep} (MPa)	0.4195	0.4195
C_{20ep} (MPa)	-0.1816	-0.1816
$C30_{ep}$ (MPa)	0.0599	0.0599
η_{Dp} (MPa/sec)	5.0	0.5

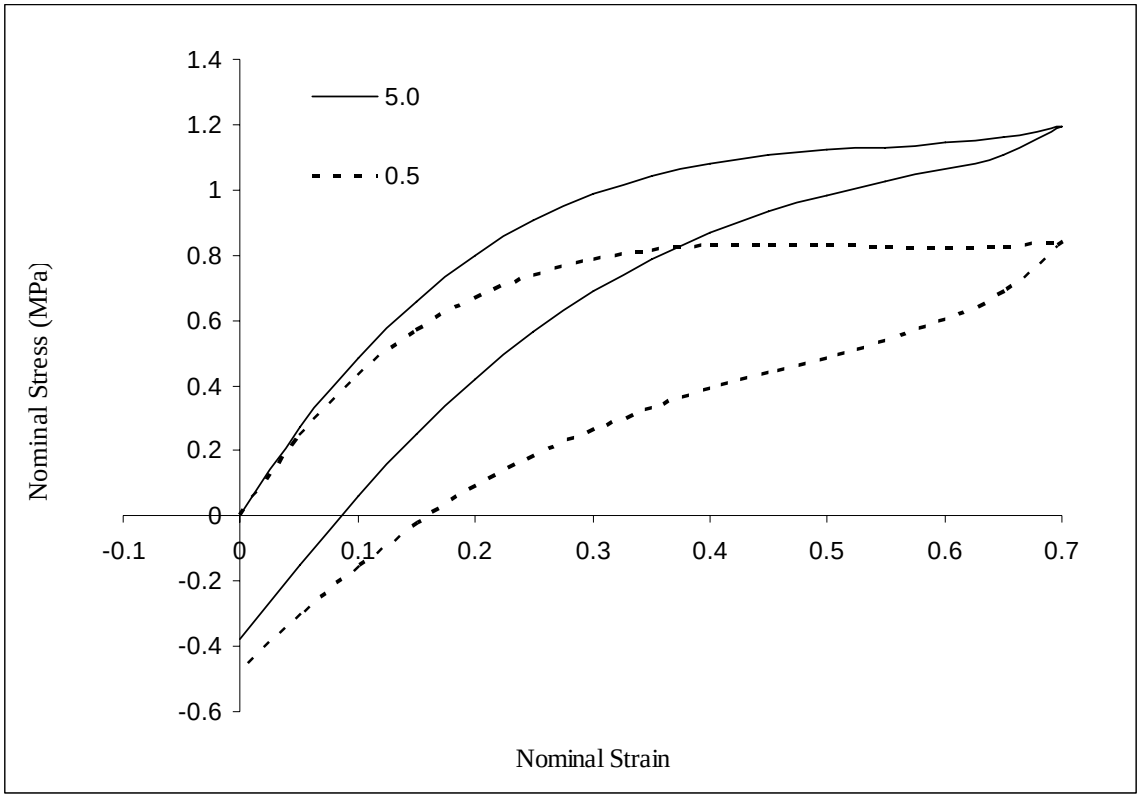

Fig. 4.12 Effect of Plastic Dissipation Constant η_{Dp} on Equilibrium Hysteresis

4.2 MATERIAL CONSTANTS DETERMINATION

In this section a procedure for fixing up the material constants is outlined. It should be noted that in reality decoupling all the behaviors to equilibrium elastic, equilibrium plastic and viscoelastic is not possible. In other words, it is not possible to obtain a unique set of constants. It is only an assumption that part of energy is spent in each mode of deformation behavior, and hence fixing up the material constants is a complicated problem. The following procedure is proposed in the thesis.

The following experiments are to be carried out for determining the material parameters

1. Uni-axial tension under quasi static conditions (1 cycle of loading-unloading)

2. Pure torsion under quasi static conditions (1 cycle of loading-unloading)
3. Uni-axial tension at different strain rates (loading only)
4. Torsion at different strain rates (loading only)
5. Relaxation test

In the present context the experimental data given in Lion (1996) is used to fit the constants. His monotonic tension experiments along with the relaxation experiment is shown in Figure 4.13

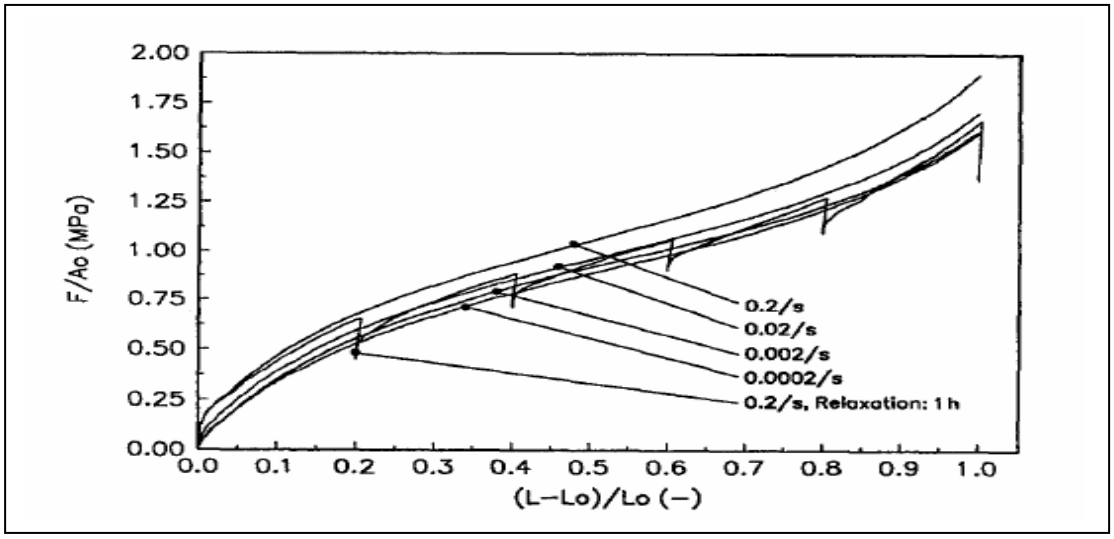

Fig. 4.13 Lion's Monotonic Tension Experiment at Different Strain Rates and the Relaxation Experiment (Lion, 1996)

Initial step in determining the material constants is to a assume trial Yeoh constants by considering the material to be non linear elastic. This can be done using standard curve fitting algorithms. To carry out this part, monotonic strain controlled experiments at a strain rate of 0.0002/sec (Figure 2.3 of Lion (1996)) is used. The Yeoh fit is shown in

Figure 4.14. From the figure, the inability of the Yeoh model to fit the experimental curve can be observed.

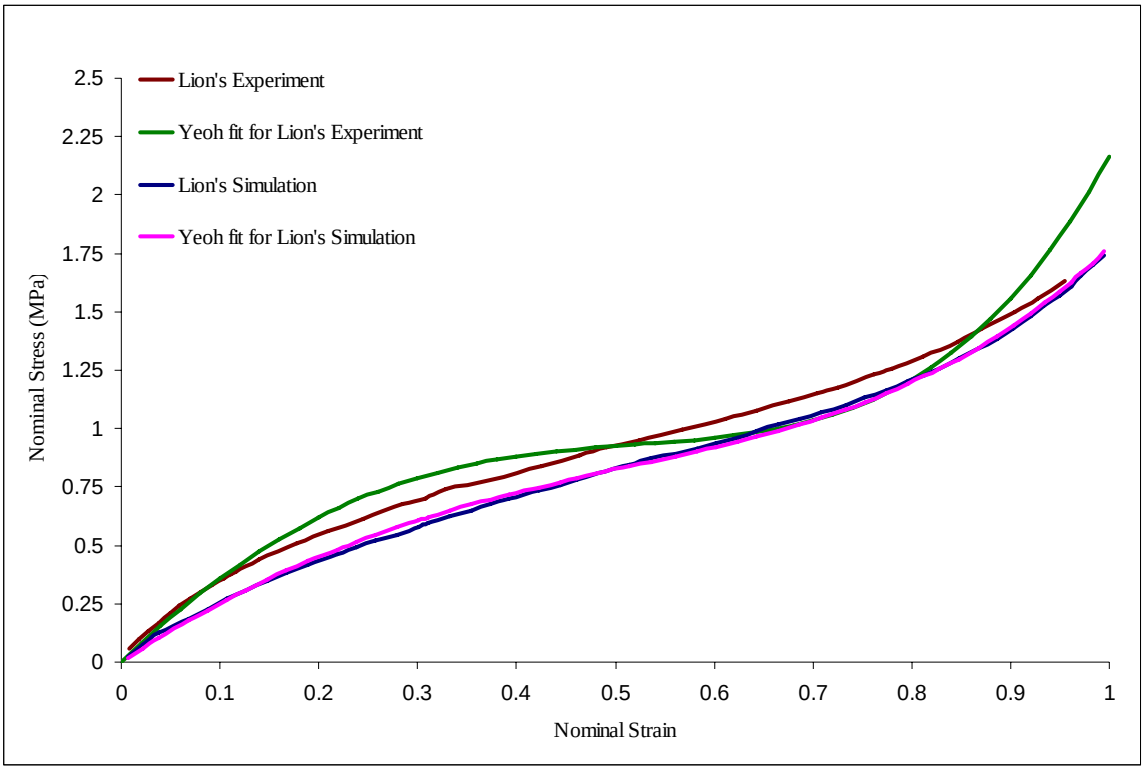

Fig. 4.14 Yeoh Fit for Lion's Experiments and the Simulations

Lion (1996) used a stored energy density function given in Equation 4.1

$$\psi = \frac{1}{2\rho}\sum_{i,j,k=1}^{3} C_{ijk}^{sp}\left(I_1-3\right)^i\left(I_2-3\right)^j\left(I_3-1\right)^k \qquad (4.1)$$

It can be noted that even this fit is in error, when compared to the experimental work. From the figure it can also be observed that Yeoh model fits very well to the numerical simulations by Lion (1996). The Yeoh constants obtained are listed in Table 4.7

Table 4.7 Fitted Yeoh constants for experiments and simulations by Lion (1996)

Constants	Constants for Experimental data	Constants for simulation data
C_{10} (MPa)	0.66754	0.4660
C_{20} (MPa)	-0.2723	-0.0959
C_{30} (MPa)	0.0866	0.0354

The next step is to fix the plastic spring constants and the value of η_{Dp} which represents equilibrium dissipation. An initial value of η_{Dp} parameter is first assumed. In the present case η_{Dp} = 1.0 MPa/sec, is assumed. Since the quasi static loading is affected mostly by the elastic and plastic springs, iteratively elastic and plastic spring constants are chosen. Since springs are present in all the modes of deformation, namely, elastic, viscoelastic and plastic, the above spring constants arrived at by considering only elastic behavior can not be used. The spring constants have to be reallocated to the plastic and viscoelastic parts. When, one considers only the quasi static loading, the viscoelastic part has no contribution and the plastic spring alone plays a role. Initially, about 20 % of the behavior is assumed to be due to plastic part. Note that, the original elastic spring constants now do not fit the curve because η_{Dp} has a value of 1.0 MPa/sec. Now the values of both the spring constants are adjusted to make the curve coincide with the experimental value. The quasi static constants obtained are listed in Table 4.8. The quasi static curve for the obtained constants in Table 4.8 is given Figure 4.15

Table 4.8 Quasi Ssatic constants

Constants	Quasi Static Constants
C_{10el} (MPa)	0.2900
C_{20el} (MPa)	-0.0479
C_{30el} (MPa)	0.0283
C_{10ep} (MPa)	0.1864
C_{20ep} (MPa)	-0.0192
C_{30ep} (MPa)	0.0213
η_{Dp} (MPa/sec)	1.0

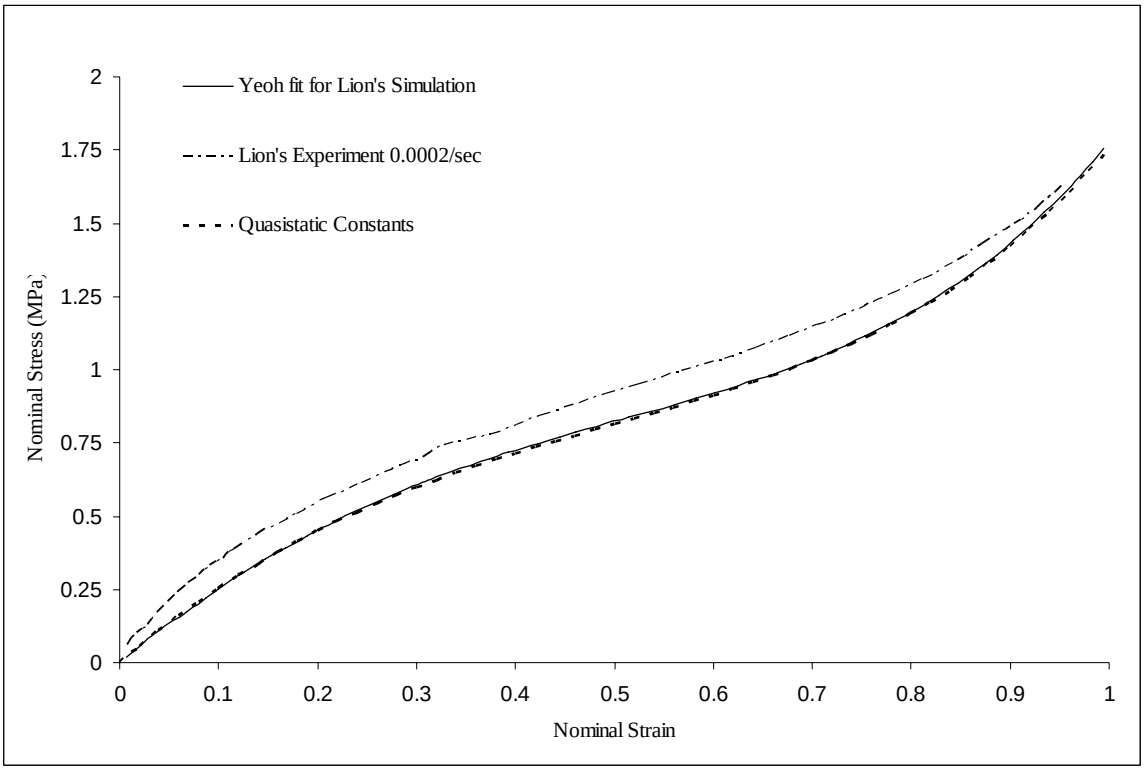

Fig. 4.15 Comparison of Quasi Static Curve with Monotonic Tension Experiment (Lion, 1996) at 0.0002/Sec Strain Rate.

The next step is to fix the η_{Dp}. This can be done by using quasi static cyclic loading curve. Since the Lion (1996) has carried out cyclic loading at a strain rate of 0.2/sec, the viscoelastic spring constant and η_{Dv} should be determined before arriving at η_{Dp} value. For this purpose, the monotonic tension experiment conducted at a strain rate of 0.2/sec is used. An initial η_{Dv} value of 1.75 MPa/sec is assumed. The spring constants are now redistributed, with an initial guess of 20 % due to the viscoelastic part. This is iteratively changed to fit the experimental curve. The resulting constants are listed in Table 4.9.

Table 4.9 Viscoelastic-plastic constants

Constants	Viscoelastic-Plastic Constatnts
C_{10el} (MPa)	0.2900
C_{20el} (MPa)	-0.0479
C_{30el} (MPa)	0.0283
C_{10ep} (MPa)	0.1864
C_{20ep} (MPa)	-0.0192
C_{30ep} (MPa)	0.0213
η_{Dp} (MPa/sec)	1.0
C_{10ev} (MPa)	0.2796
C_{20ev} (MPa)	-0.0479
C_{30ev} (MPa)	0.0354
η_{Dv} (MPa/sec)	1.75

Figure 4.16 shows the comparison between the experiment at 0.2/sec strain rate and viscoelastic-plastic material model with the obtained constants at the same rate. The viscoelastic plastic material model fits the experiment with small error as shown in the figure.

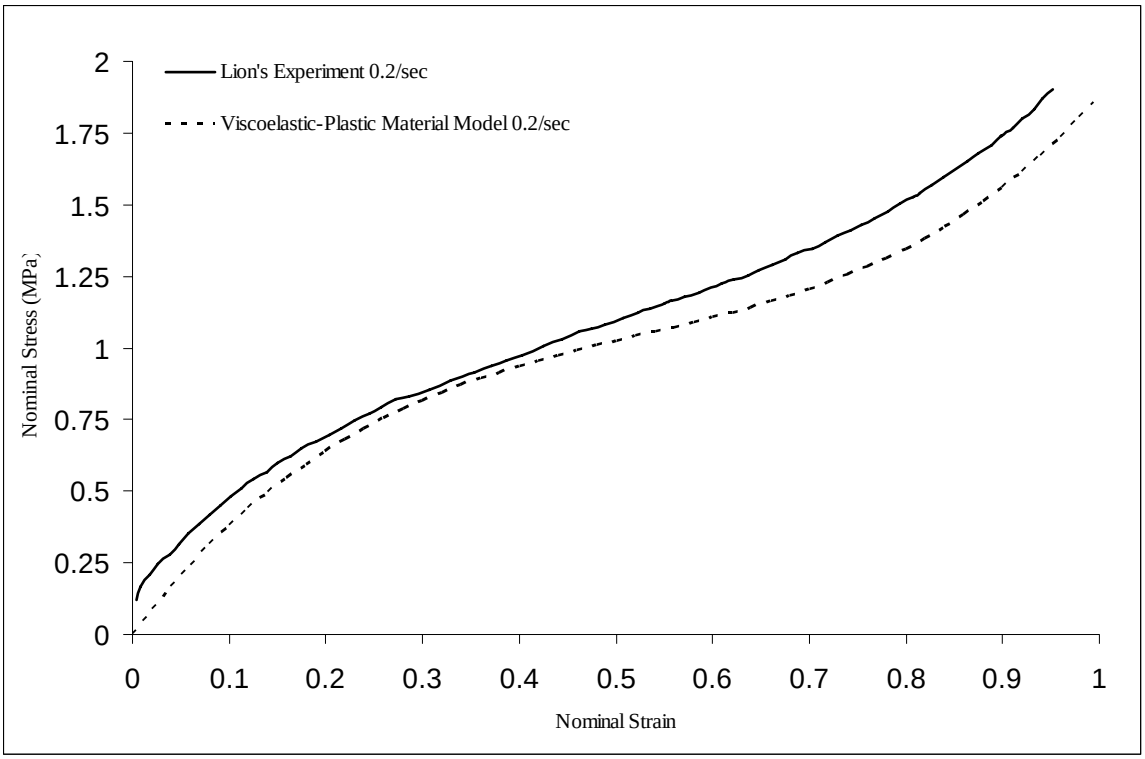

Fig. 4.16 Comparison of Viscoelastic-Plastic Material Model with Monotonic Tension Experiment (Lion, 1996) at 0.2/Sec Strain Rate

Now the η_{Dv} value is to be estimated, since the η_{Dv} value is most significant in relaxation behavior, it is to be evaluated from the relaxation experiment. The value of η_{Dv} is estimated to be 2.0 MPa/sec and the relaxation graph compared to initial η_{Dv} value of 1.75 is shown in Figure 4.17.

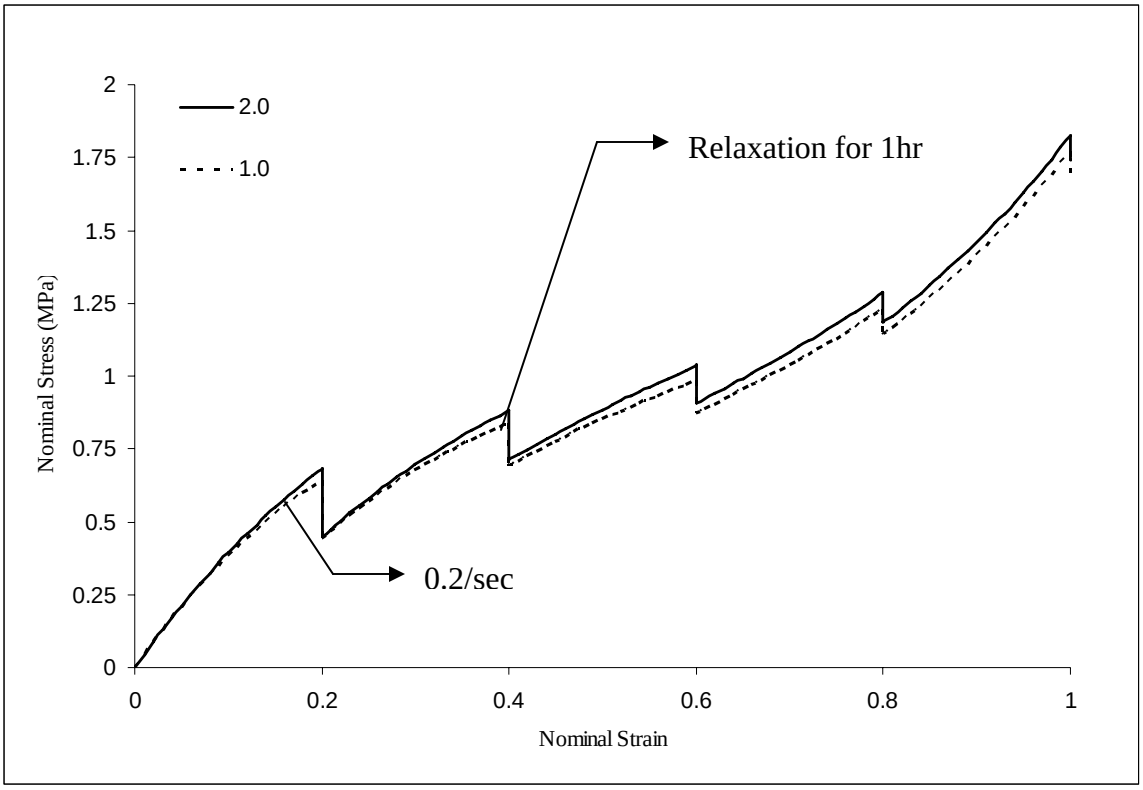

Fig. 4.17 Comparison between Two η_{Dev} Values for Step strain with relaxation

With the revised coefficient, the monotonic tension at 0.2/sec strain rate is rerun to compare with the experimental data and is shown in Figure 4.18.

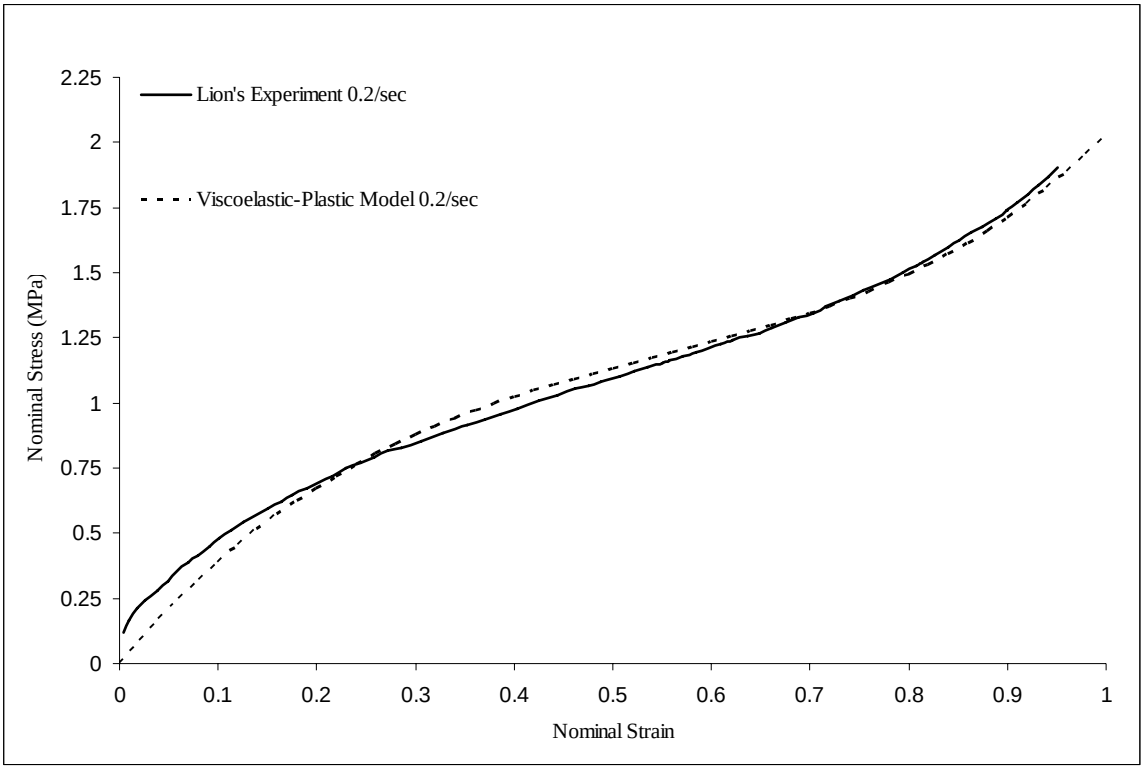

Fig. 4.18 Comparison of Viscoelastic-Plastic Material Model using updated η_{Dv} Under Monotonic Tension Experiment (Lion, 1996) at 0.2/Sec Strain Rate

Finally η_{Dp} is to be determined. η_{Dp} has a significant effect on the equilibrium dissipation. For this the cyclic loading curve at a rate of 0.2/sec with a mean strain of 0.0 and with an amplitude of 0.3 (Lion, 1996) is used. The value of η_{Dp} is estimated to be 0.75 MPa/sec. Figure 4.19 shows the difference between an initial assumed η_{Dp} = 1.0 MPa/sec and η_{Dp} = 0.75 MPa/sec. Even though the graph looks to be similar the equilibrium hysteresis is slightly higher with η_{Dp} = 0.75 MPa/sec

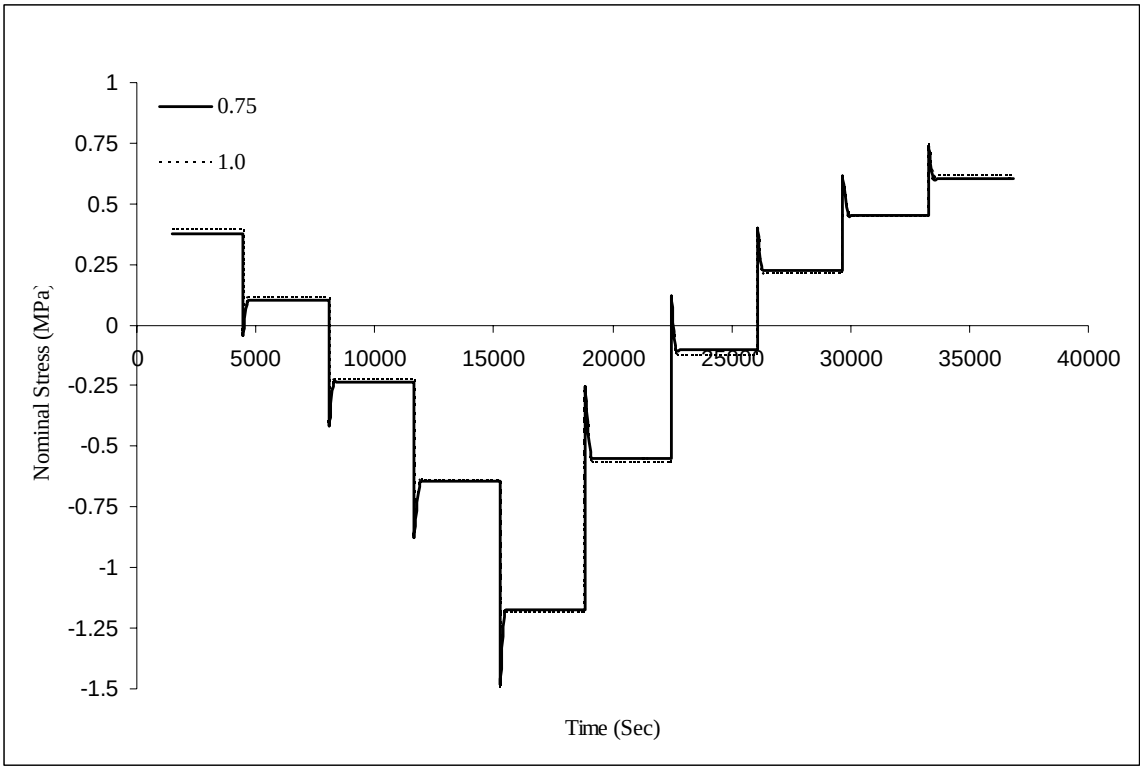

Fig. 4.18 Cyclic Loading Experiment: Comparison different η_{Dp} values

Figure 4.20 shows the comparison with the experimental data. If the material model is assumed to be only viscoelastic the equilibrium hysteresis which is observed in the experiment can't be represented. The viscoelastic material is also plotted for comparison in the figure. The equilibrium hysteresis measured as the difference in stress at the same strain level, in Lion's experiment at 18% strain it is 0.09Mpa while in the developed viscoelastic-plastic model it is 0.095 Mpa.

The final constants for viscoelastic-plastic material model and the viscoelastic material model are listed in Table 4.10.

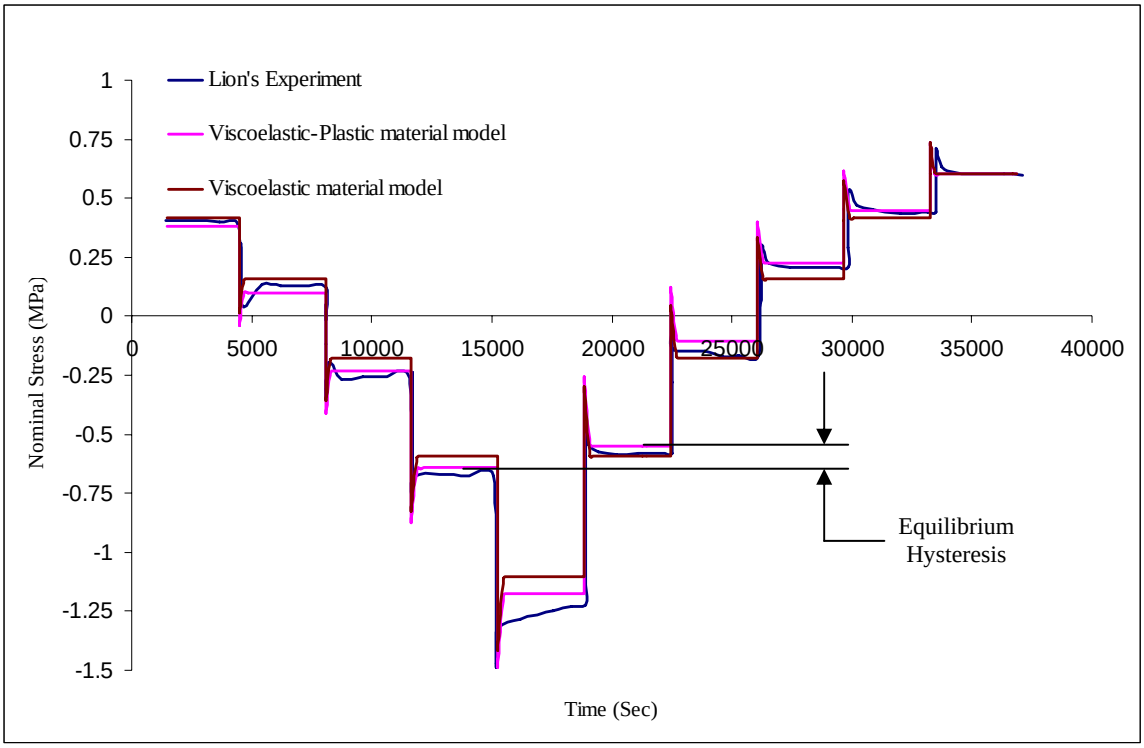

Fig. 4.20 Cyclic Loading Experiment: Comparison among the Experiment, Viscoelastic-Plastic and Viscoelastic Material Models.

Table 4.10 Final Viscoelastic-plastic constants and Viscoelastic constants

Constants	Final Constants for Viscoelastic-Plastic Material Model	Final Constants for Viscoelastic Material Model
C_{10el} (MPa)	0.2900	0.466
C_{20el} (MPa)	-0.0479	-0.0959
C_{30el} (MPa)	0.0283	0.0353
C_{10ep} (MPa)	0.1864	------
C_{20ep} (MPa)	-0.0192	------
C_{30ep} (MPa)	0.0213	------
η_{Dp} (MPa/sec)	1.0	------
C_{10ev} (MPa)	0.2796	0.2796
C_{20ev} (MPa)	-0.0479	-0.0479
C_{30ev} (MPa)	0.0354	0.0354
η_{Dv} (MPa/sec)	2.0	2.0

4.3 Comparison with Reese and Govindjee Model

In this section the viscoelstic constitutive model is compared with Reese and Govindjee (1998a). In their work all the simulations use Ogden strain energy function for elastic as well as viscoelastic parts.

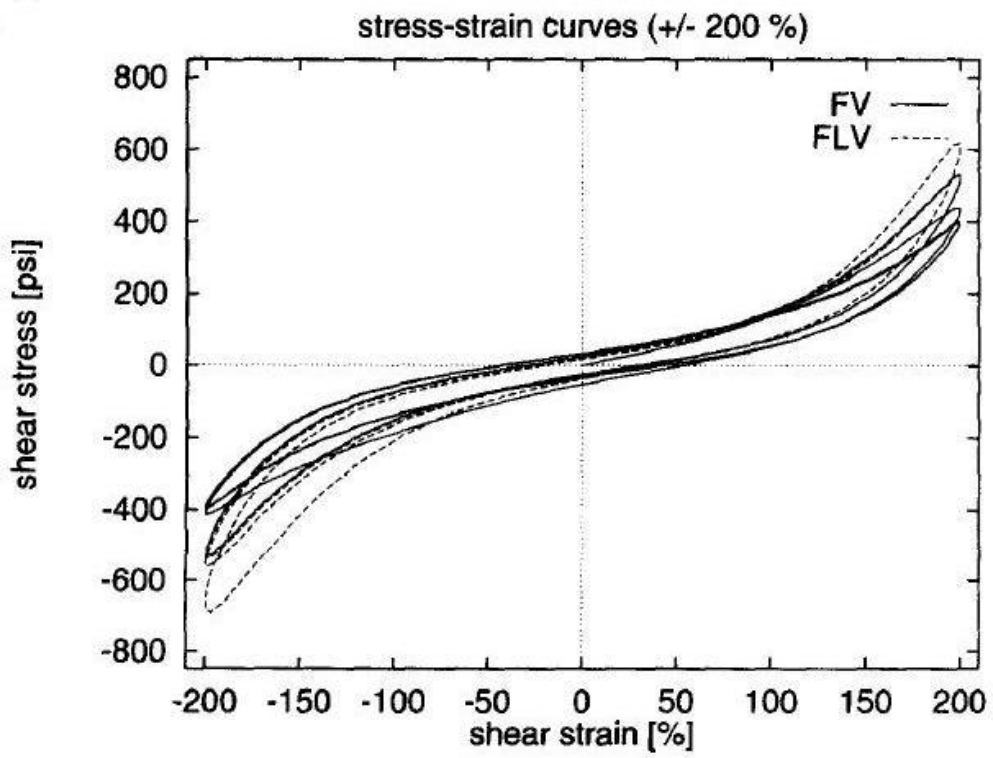

Fig. 4.21 Shear test: Stress-Strain Curve at ±200% (Reese and Govindjee, 1998a)

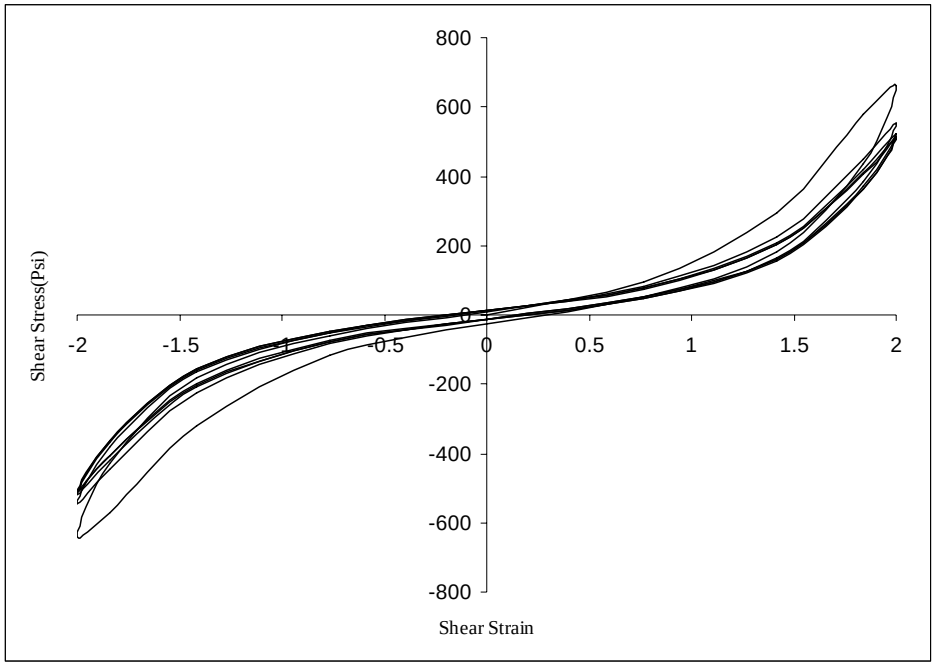

Fig. 4.22 Shear test: Stress-Strain Curve at ±200% with viscoelastic constitutive relation and Yeoh strain energy function

4.4 SUMMARY

The developed material model is studied for the sensitivity of the material parameters involved. Procedure for deriving material constants is also described. Material constants were derived for the test data given in Lion (1996). The developed material model is compared with the test data under complex loading conditions. The viscoelastic constitutive relation is compared to Reese and Govindjee (1998a) shear tests.

CHAPTER 5

CONCLUSIONS

5.1 CONTRIBUTION

A viscoelastic-plastic constitutive model is developed based on the multiplicative decomposition of the deformation gradient and the additive decomposition of the total stored energy into elastic, viscoelastic and plastic parts. The developed material model is suitable for elastomers, wherein, the material shows rate dependent and rate independent hysteresis. The predictor - corrector algorithm is proposed for numerical implementation which is very efficient, simple and is easy to implement. The constitutive model has been implemented in ABAQUS through user material subroutine UMAT. The step by step algorithm for UMAT is given.

5.2 CONCLUSIONS

The following are the conclusions with the developed viscoelastic-plastic constitutive model.

1. The shape of the stress-strain curve is decided by elastic part of the stored energy density function.
2. The total dissipation is a function of spring constants of viscoelastic and plastic parts as well as η_{Dv} η_{Dp} parameters.

3. It is possible to derive a procedure for determining the material constants.
4. It is possible to estimate the total dissipation in the deformation processes

5.3 FUTURE SCOPE OF THE WORK

1. The proposed constitutive model can be extended to include temperature effects.
2. The developed constitutive model can also be applied for finding the rolling resistance in an automobile tire.

APPENDIX-A

DETAILED EXPRESSIONS FOR YEOH MODEL

A.1 CAUCHY STRESS FOR YEOH HYPERELASTIC MODEL

The Yeoh form of the strain energy function can be given by

$$\psi = \psi_{iso} + \psi_{vol} = C_{10}\left(\bar{I}_1 - 3\right) + C_{20}\left(\bar{I}_1 - 3\right)^2 + C_{30}\left(\bar{I}_1 - 3\right)^3 + \frac{1}{D}\left(J-1\right)^2 \tag{A.1}$$

Where $\bar{I}_1$ the first invariant of the left Cauchy deformation tensor

$$\bar{I}_1 = J^{-\frac{2}{3}}\left(\lambda_1^2 + \lambda_2^2 + \lambda_3^2\right) \tag{A.2}$$

$$J = \lambda_1\lambda_2\lambda_3 \tag{A.3}$$

Kirchoff stress in principal space is given by

$$\tau_A = \lambda_A \frac{\partial \psi}{\partial \lambda_A} \tag{A.4}$$

$$\left[\tau_A\right]_{iso} = \frac{\partial \psi_{iso}}{\partial \lambda_A} = \lambda_A \frac{\partial \psi_{iso}}{\partial \bar{I}_1}\frac{\partial \bar{I}_1}{\partial \lambda_A} \tag{A.5}$$

$$\frac{\partial \psi_{iso}}{\partial \bar{I}_1} = C_{10} + 2C_{20}\left(\bar{I}_1 - 3\right) + 3C_{30}\left(\bar{I}_1 - 3\right)^2 \tag{A.6}$$

$$\begin{aligned}\frac{\partial \bar{I}_1}{\partial \lambda_A} &= J^{-\frac{2}{3}}2\lambda_A + \left(\lambda_1^2 + \lambda_2^2 + \lambda_3^2\right)\left(-\frac{2}{3}\right)J^{-\frac{5}{3}+1}\frac{1}{\lambda_A} \\ &= 2J^{-\frac{2}{3}}\lambda_A - \frac{2}{3}\frac{1}{\lambda_A}J^{-\frac{2}{3}}I_1 = 2J^{-\frac{2}{3}}\frac{1}{\lambda_A}\left(\lambda_A^2 - \frac{1}{3}I_1\right)\end{aligned} \tag{A.7}$$

$$\begin{aligned}\left[\tau_A\right]_{iso} &= \lambda_A \frac{\partial \psi_{iso}}{\partial \bar{I}_1}\frac{\partial \bar{I}_1}{\partial \lambda_A} \\ &= 2J^{-\frac{2}{3}}\left(\lambda_A^2 - \frac{1}{3}I_1\right)\left(C_{10} + 2C_{20}\left(\bar{I}_1 - 3\right) + 3C_{30}\left(\bar{I}_1 - 3\right)^2\right)\end{aligned} \tag{A.8}$$

The deviatoric part of the Cauchy stress is given by

$$\left[\sigma_A\right]_{iso} = \frac{1}{J}\left[\tau_A\right]_{iso} = 2J^{-\frac{5}{3}}\left(\lambda_A^2 - \frac{1}{3}I_1\right)\left(C_{10} + 2C_{20}\left(\bar{I}_1 - 3\right) + 3C_{30}\left(\bar{I}_1 - 3\right)^2\right) \tag{A.9}$$

The volumetric part of the Cauchy stress is given by

$$\left[\sigma_A\right]_{vol} = \frac{d\psi_{vol}}{dJ} = \frac{2}{D}\left(J - 1\right)\right) \tag{A.10}$$

The total Cauchy stress is given by

$$\left[\sigma_A\right]_{total} = \left[\sigma_A\right]_{iso} + \left[\sigma_A\right]_{vol} \tag{A.11}$$

$$\left[\sigma_A\right]_{total} = 2J^{-\frac{5}{3}}\left(\lambda_A^2 - \frac{1}{3}I_1\right)\left(C_{10} + 2C_{20}\left(\bar{I}_1 - 3\right) + 3C_{30}\left(\bar{I}_1 - 3\right)^2\right) + \frac{2}{D}\left(J - 1\right) \tag{A.12}$$

A.2 SPATIAL TANGENT MODULI FOR YEOH MODEL

Now the spatial tangent moduli is to be calculated. It is also decomposed into isochoric and volumetric parts. The isochoric part of the tangent moduli is given by (Zienkiewicz and Taylor, 2000)

$$\left(c_{IJKL}\right)_{iso} = \frac{1}{J}\left\{\begin{array}{l}\left(\sum_{M=1}^{3}\sum_{N=1}^{3}\frac{\partial \psi}{\partial \varepsilon_M \partial \varepsilon_N} - 2\tau_M \delta_{MN}\right) N_I^M N_J^M N_K^N N_L^N \\ + \sum_{\substack{M=1 \\ M\neq N}}^{3}\sum_{N=1}^{3} g_{MN}\left(N_I^M N_J^N N_K^M N_L^N + N_I^M N_J^N N_K^N N_L^M\right)\end{array}\right\} \tag{A.13}$$

Where $\varepsilon_M = \ln\left(\lambda_M\right)$ (A.14)

$$g_{MN}=\begin{cases}\dfrac{\tau_M\lambda_N^2-\tau_N\lambda_M^2}{\lambda_M^2-\lambda_N^2};\lambda_M\neq\lambda_N\\ \dfrac{\partial\left(\tau_M-\tau_N\right)}{\partial\varepsilon_M};\lambda_M=\lambda_N\end{cases} \tag{A.15}$$

Now $\dfrac{\partial\psi}{\partial\varepsilon_M\partial\varepsilon_N}$ is to be calculated

$$\frac{\partial\psi}{\partial\varepsilon_M\partial\varepsilon_N}=\frac{\partial\tau_M}{\partial\varepsilon_N}=\lambda_M\frac{\partial\tau_M}{\partial\lambda_N} \tag{A.16}$$

$$\begin{aligned}\frac{\partial\tau_A}{\partial\lambda_B}&=2J^{-\frac{2}{3}}\left(\lambda_A^2-\frac{1}{3}I_1\right)\left(2C_{20}+6C_{30}\left(\bar{I}_1-3\right)\right)\frac{\partial\bar{I}_1}{\partial\lambda_B}\\&+2J^{-\frac{2}{3}}\left(C_{10}+2C_{20}\left(\bar{I}_1-3\right)+3C_{30}\left(\bar{I}_1-3\right)^2\right)\left(2\lambda_A\delta_{AB}-\frac{1}{3}2\lambda_B\right)\\&+2\left(\lambda_A^2-\frac{1}{3}I_1\right)\left(C_{10}+2C_{20}\left(\bar{I}_1-3\right)+3C_{30}\left(\bar{I}_1-3\right)^2\right)\left(-\frac{2}{3}\right)J^{-\frac{2}{3}}\frac{1}{\lambda_B}\end{aligned} \tag{A.17}$$

$$\begin{aligned}\frac{\partial\tau_A}{\partial\lambda_B}&=2J^{-\frac{2}{3}}\left(\lambda_A^2-\frac{1}{3}I_1\right)\left(2C_{20}+6C_{30}\left(\bar{I}_1-3\right)\right)\left(2J^{-\frac{2}{3}}\frac{1}{\lambda_B}\left(\lambda_B^2-\frac{1}{3}I_1\right)\right)\\&+2J^{-\frac{2}{3}}\left(C_{10}+2C_{20}\left(\bar{I}_1-3\right)+3C_{30}\left(\bar{I}_1-3\right)^2\right)\left(2\lambda_A\delta_{AB}-\frac{1}{3}2\lambda_B\right)\\&+2\left(\lambda_A^2-\frac{1}{3}I_1\right)\left(C_{10}+2C_{20}\left(\bar{I}_1-3\right)+3C_{30}\left(\bar{I}_1-3\right)^2\right)\left(-\frac{2}{3}\right)J^{-\frac{2}{3}}\frac{1}{\lambda_B}\end{aligned} \tag{A.18}$$

$$\frac{\partial\tau_A}{\partial\lambda_B}=2J^{-\frac{2}{3}}\frac{1}{\lambda_B}\begin{bmatrix}2J^{-\frac{2}{3}}\left(\lambda_A^2-\frac{1}{3}I_1\right)\left(\lambda_B^2-\frac{1}{3}I_1\right)\left(C_{10}+2C_{20}\left(\bar{I}_1-3\right)+3C_{30}\left(\bar{I}_1-3\right)^2\right)\\+2\left(C_{10}+2C_{20}\left(\bar{I}_1-3\right)+3C_{30}\left(\bar{I}_1-3\right)^2\right)\left(\lambda_A\lambda_B\delta_{AB}-\frac{1}{3}\lambda_B^2\right)\\-\frac{2}{3}\left(\lambda_A^2-\frac{1}{3}I_1\right)\left(C_{10}+2C_{20}\left(\bar{I}_1-3\right)+C_{30}\left(\bar{I}_1-3\right)^2\right)\end{bmatrix} \tag{A.19}$$

$$\frac{\partial \tau_A}{\partial \lambda_B} = \frac{4}{9}\frac{1}{\lambda_B}\begin{bmatrix} \left(3\bar{\lambda}_A^2 - \bar{I}_1\right)\left(3\bar{\lambda}_B^2 - \bar{I}_1\right)\left(C_{10} + 2C_{20}\left(\bar{I}_1 - 3\right) + 3C_{30}\left(\bar{I}_1 - 3\right)^2\right) \\ + \left(C_{10} + 2C_{20}\left(\bar{I}_1 - 3\right) + 3C_{30}\left(\bar{I}_1 - 3\right)^2\right)\left(9\bar{\lambda}_A\bar{\lambda}_B\delta_{AB} - 3\bar{\lambda}_B^2\right) \\ - \left(3\bar{\lambda}_A^2 - \bar{I}_1\right)\left(C_{10} + 2C_{20}\left(\bar{I}_1 - 3\right) + C_{30}\left(\bar{I}_1 - 3\right)^2\right) \end{bmatrix} \tag{A.20}$$

$$\frac{\partial \psi}{\partial \varepsilon_A \partial \varepsilon_B} = \lambda_B \frac{\partial \tau_A}{\partial \lambda_B} = \frac{4}{9}\begin{bmatrix} \left(3\bar{\lambda}_A^2 - \bar{I}_1\right)\left(3\bar{\lambda}_B^2 - \bar{I}_1\right)\left(C_{10} + 2C_{20}\left(\bar{I}_1 - 3\right) + 3C_{30}\left(\bar{I}_1 - 3\right)^2\right) \\ + \left(C_{10} + 2C_{20}\left(\bar{I}_1 - 3\right) + 3C_{30}\left(\bar{I}_1 - 3\right)^2\right)\left(9\bar{\lambda}_A\bar{\lambda}_B\delta_{AB} - 3\bar{\lambda}_B^2\right) \\ - \left(3\bar{\lambda}_A^2 - \bar{I}_1\right)\left(C_{10} + 2C_{20}\left(\bar{I}_1 - 3\right) + C_{30}\left(\bar{I}_1 - 3\right)^2\right) \end{bmatrix}$$

(A.21)

$$\begin{aligned} \frac{\partial \tau_A}{\partial \lambda_A} &= 2J^{-\frac{2}{3}}\left(\lambda_A^2 - \frac{1}{3}I_1\right)\left(2C_{20} + 6C_{30}\left(\bar{I}_1 - 3\right)\right)\frac{\partial \bar{I}_1}{\partial \lambda_A} \\ &+ 2J^{-\frac{2}{3}}\left(C_{10} + 2C_{20}\left(\bar{I}_1 - 3\right) + 3C_{30}\left(\bar{I}_1 - 3\right)^2\right)\left(2\lambda_A - \frac{1}{3}2\lambda_A\right) \\ &+ 2\left(\lambda_A^2 - \frac{1}{3}I_1\right)\left(C_{10} + 2C_{20}\left(\bar{I}_1 - 3\right) + 3C_{30}\left(\bar{I}_1 - 3\right)^2\right)\left(-\frac{2}{3}\right)J^{-\frac{2}{3}}\frac{1}{\lambda_A} \end{aligned} \tag{A.22}$$

$$\begin{aligned} \frac{\partial \tau_A}{\partial \lambda_A} &= 2J^{-\frac{2}{3}}\left(\lambda_A^2 - \frac{1}{3}I_1\right)\left(2C_{20} + 6C_{30}\left(\bar{I}_1 - 3\right)\right)\left(2J^{-\frac{2}{3}}\frac{1}{\lambda_A}\left(\lambda_A^2 - \frac{1}{3}I_1\right)\right) \\ &+ 2J^{-\frac{2}{3}}\left(C_{10} + 2C_{20}\left(\bar{I}_1 - 3\right) + 3C_{30}\left(\bar{I}_1 - 3\right)^2\right)\left(\frac{4}{3}\lambda_A\right) \\ &+ 2\left(\lambda_A^2 - \frac{1}{3}I_1\right)\left(C_{10} + 2C_{20}\left(\bar{I}_1 - 3\right) + 3C_{30}\left(\bar{I}_1 - 3\right)^2\right)\left(-\frac{2}{3}\right)J^{-\frac{2}{3}}\frac{1}{\lambda_A} \end{aligned} \tag{A.23}$$

$$\frac{\partial \tau_A}{\partial \lambda_A} = 2J^{-\frac{2}{3}} \frac{1}{\lambda_A} \begin{bmatrix} 2J^{-\frac{2}{3}} \left(\lambda_A^2 - \frac{1}{3} I_1 \right)^2 \left(C_{10} + 2C_{20} \left(\bar{I}_1 - 3 \right) + 3C_{30} \left(\bar{I}_1 - 3 \right)^2 \right) \\ + \frac{2}{3} \lambda_A \left(C_{10} + 2C_{20} \left(\bar{I}_1 - 3 \right) + 3C_{30} \left(\bar{I}_1 - 3 \right)^2 \right) \\ - \frac{2}{3} \left(\lambda_A^2 - \frac{1}{3} I_1 \right) \left(C_{10} + 2C_{20} \left(\bar{I}_1 - 3 \right) + C_{30} \left(\bar{I}_1 - 3 \right)^2 \right) \end{bmatrix} \tag{A.24}$$

$$\frac{\partial \tau_A}{\partial \lambda_A} = \frac{4}{9} \frac{1}{\lambda_A} \begin{bmatrix} \left(3\bar{\lambda}_A^2 - \bar{I}_1 \right)^2 \left(C_{10} + 2C_{20} \left(\bar{I}_1 - 3 \right) + 3C_{30} \left(\bar{I}_1 - 3 \right)^2 \right) \\ + 3\bar{\lambda}_A^2 \left(C_{10} + 2C_{20} \left(\bar{I}_1 - 3 \right) + 3C_{30} \left(\bar{I}_1 - 3 \right)^2 \right) \\ - \left(3\bar{\lambda}_A^2 - I_1 \right) \left(C_{10} + 2C_{20} \left(\bar{I}_1 - 3 \right) + C_{30} \left(\bar{I}_1 - 3 \right)^2 \right) \end{bmatrix} \tag{A.25}$$

$$\begin{aligned} \frac{\partial \tau_A}{\partial \varepsilon_A} - \frac{\partial \tau_B}{\partial \varepsilon_A} = & \frac{4}{9} \begin{bmatrix} \left(3\bar{\lambda}_A^2 - \bar{I}_1 \right)^2 \left(C_{10} + 2C_{20} \left(\bar{I}_1 - 3 \right) + 3C_{30} \left(\bar{I}_1 - 3 \right)^2 \right) \\ + 3\bar{\lambda}_A^2 \left(C_{10} + 2C_{20} \left(\bar{I}_1 - 3 \right) + 3C_{30} \left(\bar{I}_1 - 3 \right)^2 \right) \\ - \left(3\bar{\lambda}_A^2 - I_1 \right) \left(C_{10} + 2C_{20} \left(\bar{I}_1 - 3 \right) + C_{30} \left(\bar{I}_1 - 3 \right)^2 \right) \end{bmatrix} \\ & - \frac{4}{9} \begin{bmatrix} \left(3\bar{\lambda}_A^2 - \bar{I}_1 \right) \left(3\bar{\lambda}_B^2 - \bar{I}_1 \right) \left(C_{10} + 2C_{20} \left(\bar{I}_1 - 3 \right) + 3C_{30} \left(\bar{I}_1 - 3 \right)^2 \right) \\ + \left(C_{10} + 2C_{20} \left(\bar{I}_1 - 3 \right) + 3C_{30} \left(\bar{I}_1 - 3 \right)^2 \right) \left(9\bar{\lambda}_A \bar{\lambda}_B \delta_{AB} - 3\bar{\lambda}_B^2 \right) \\ - \left(3\bar{\lambda}_B^2 - \bar{I}_1 \right) \left(C_{10} + 2C_{20} \left(\bar{I}_1 - 3 \right) + C_{30} \left(\bar{I}_1 - 3 \right)^2 \right) \end{bmatrix} \end{aligned} \tag{A.26}$$

For $\boldsymbol{\lambda_A = \lambda_B}$

$$\begin{aligned} \frac{\partial \tau_A}{\partial \varepsilon_A} - \frac{\partial \tau_B}{\partial \varepsilon_A} = & \frac{4}{9} \left[3\bar{\lambda}_A^2 \left(C_{10} + 2C_{20} \left(\bar{I}_1 - 3 \right) + 3C_{30} \left(\bar{I}_1 - 3 \right)^2 \right) \right] \\ & - \frac{4}{9} \left[+ \left(C_{10} + 2C_{20} \left(\bar{I}_1 - 3 \right) + 3C_{30} \left(\bar{I}_1 - 3 \right)^2 \right) \left(6\bar{\lambda}_A^2 \right) \right] \end{aligned} \tag{A.27}$$

$$\frac{\partial \tau_A}{\partial \varepsilon_A} - \frac{\partial \tau_B}{\partial \varepsilon_A} = -\frac{4}{3} \left[\bar{\lambda}_A^2 \left(C_{10} + 2C_{20} \left(\bar{I}_1 - 3 \right) + 3C_{30} \left(\bar{I}_1 - 3 \right)^2 \right) \right] \tag{A.28}$$

The volumetric part of the spatial tangent moduli is given by

$$\left(c_{IJKL} \right)_{vol} = \bar{p}_{IM} \delta_{MJ} \delta_{KL} - 2 p_{IN} \delta_{NK} \delta_{JL} \tag{A.29}$$

Where

$$\bar{p}_{IJ} = p_{IJ} + J\frac{\partial p_{IJ}}{\partial J} \text{ and } p_{IJ} = \frac{\partial \psi_{vol}}{\partial J}\delta_{IJ} \tag{A.30}$$

$$\frac{\partial p_{IJ}}{\partial J} = \frac{2}{D}\delta_{IJ} \tag{A.31}$$

When $\lambda_m \neq \lambda_n$ the isochoric part of the spatial tangent modli is given by

$$\left(c_{IJKL}\right)_{iso} = \frac{1}{J}\left\{\begin{array}{l}\left(\begin{array}{l}\sum_{M=1}^{3}\sum_{N=1}^{3}\frac{4}{9}\left[\begin{array}{l}\left(3\bar{\lambda}_M^2 - \bar{I}_1\right)\left(3\bar{\lambda}_N^2 - \bar{I}_1\right)\left(C_{10} + 2C_{20}\left(\bar{I}_1 - 3\right) + 3C_{30}\left(\bar{I}_1 - 3\right)^2\right) \\ + \left(C_{10} + 2C_{20}\left(\bar{I}_1 - 3\right) + 3C_{30}\left(\bar{I}_1 - 3\right)^2\right)\left(9\bar{\lambda}_M\bar{\lambda}_N\delta_{MN} - 3\bar{\lambda}_N^2\right) \\ -\left(3\bar{\lambda}_M^2 - \bar{I}_1\right)\left(C_{10} + 2C_{20}\left(\bar{I}_1 - 3\right) + C_{30}\left(\bar{I}_1 - 3\right)^2\right)\end{array}\right] \\ -4J^{-\frac{2}{3}}\left(\lambda_M^2 - \frac{1}{3}I_1\right)\left(C_{10} + 2C_{20}\left(\bar{I}_1 - 3\right) + 3C_{30}\left(\bar{I}_1 - 3\right)^2\right)\delta_{MN}\end{array}\right) \\ N_I^M N_J^M N_K^N N_L^N \\ +\sum_{M=1}^{3}\sum_{\substack{N=1 \\ M\neq N}}^{3}\frac{\tau_M\lambda_n^2 - \tau_N\lambda_M^2}{\lambda_M^2 - \lambda_N^2}\left(N_I^M N_J^N N_K^M N_L^N + N_I^M N_J^N N_K^N N_L^M\right)\end{array}\right. \tag{A.32}$$

When $\lambda_A = \lambda_B$ the isochoric part of the spatial tangent modli is given by

$$
\left(c_{IJKL}\right)_{iso} = \frac{1}{J}\left\{
\begin{array}{l}
\left(
\begin{array}{l}
\sum_{M=1}^{3}\sum_{N=1}^{3}\frac{4}{9}\left[
\begin{array}{l}
\left(3\bar{\lambda}_M^2 - \bar{I}_1\right)\left(3\bar{\lambda}_N^2 - \bar{I}_1\right)\left(C_{10} + 2C_{20}\left(\bar{I}_1 - 3\right) + 3C_{30}\left(\bar{I}_1 - 3\right)^2\right) \\
+\left(C_{10} + 2C_{20}\left(\bar{I}_1 - 3\right) + 3C_{30}\left(\bar{I}_1 - 3\right)^2\right)\left(9\bar{\lambda}_M\bar{\lambda}_N\delta_{MN} - 3\bar{\lambda}_N^2\right) \\
-\left(3\bar{\lambda}_M^2 - \bar{I}_1\right)\left(C_{10} + 2C_{20}\left(\bar{I}_1 - 3\right) + C_{30}\left(\bar{I}_1 - 3\right)^2\right)
\end{array}
\right] \\
-4J^{-\frac{2}{3}}\left(\lambda_M^2 - \frac{1}{3}I_1\right)\left(C_{10} + 2C_{20}\left(\bar{I}_1 - 3\right) + 3C_{30}\left(\bar{I}_1 - 3\right)^2\right)\delta_{MN}
\end{array}
\right) \\
N_I^M N_J^M N_K^N N_L^N \\
+\sum_{M=1}^{3}\sum_{\substack{N=1 \\ M\neq N}}^{3}\left(-\frac{4}{3}\left[\bar{\lambda}_M^2\left(C_{10} + 2C_{20}\left(\bar{I}_1 - 3\right) + 3C_{30}\left(\bar{I}_1 - 3\right)^2\right)\right]\right) \\
+\sum_{M=1}^{3}\sum_{\substack{N=1 \\ M\neq N}}^{3}\left(N_I^M N_J^N N_K^M N_L^N + N_I^M N_J^N N_K^N N_L^M\right)
\end{array}
\right\}
\tag{A.33}
$$

REFERENCES

1. **ABAUQS,** *ABAQUS Version 6.5 Documentation*. ABQUS INC., Providence, RI, 2005.

2. **Arruda, E. M. and M. C. Boyce** (1993), A three-dimensional constitutive model for the large stretch behavior of rubber elastic materials. *Journal of the mechanics and physics of solids,* **41**, 389-412.

3. **Belytschko, T., W. K. Liu and B. Moran** *Nonlinear Finite Elements for Continua and Structures*. John wiley & sons, Ltd., 2000.

4. **Bergstrom, J.S. and M. C. Boyce** (1998), Constitutive modeling of the large strain time dependent behavior of elastomers. *Journal of the mechanics and physics of solids,* **46**, 931-954.

5. **Bonet, J.** (2001), Large strain viscoelastic constitutive models, *International journal of solids and structures.* **38**, 2953-2968.

6. **Bueche, F.** (1960)**,** Molecular basis for Mullins effect. *Journal applied polymer science.* **4**, 107-114.

7. **Christensen, R. M. (**1980), A nonlinear theory of viscoelasticity for application to elastomers. *Transactions of the ASME,* **47**, 762-768.

8. **Coleman, B.D., and M. E. Gurtin** (1967), Thermodynamics with internal state variables. *The journal of chemical physics*, **47**, 597-613.

9. **Genta, G.** *Motor Vehicle Dynamics-Modeling and Simulation,* World Scientific, Singapore, 1997.

10. **Govindjee, S., and J. C. Simo** (1991), A micro-mechanically based continuum damage model for carbon black-filled rubbers incorporating the Mullins effect. *Journal of mechanics and physics of solids*, **39**, 87-112.

11. **Govindjee, S., and J. C. Simo** (1992), Transition from micro-mechanics to computationally efficient phenomenology carbon black filled rubbers incorporating Mullins effect. *Journal of mechanics and physics of solids*, **40**, 213-233.

12. **Haupt, P**, *Continuum Mechanics and Theory of Materials*, Springer-Verlag Berlin Heidelberg New York, 2000.

13. **Haupt, P. and A. Lion** (2002), On finite linear viscoelasticity of incompressible isotropic materials. *Acta mechanica*, **159**, 87-124.

14. **Haupt, P. and K. Sedlan** (2001), Viscoplasticity of elastomeric materials: experimental facts and constitutive modeling. *Archive of applied mechanics*, **71**, 89-109.

15. **Holownia, B. P. and E. H. James** (1993), Determination of dynamic bulk modulus of elastomers using pressure measurement. *Rubber chemistry and technology*, **66**, 749-753.

16. **Holzapfel G.A.** *Nonlinear Solid Mechanics*. John wiley & sons, Ltd., 2000.

17. **Holzapfel G.A.** (1996), On large strain vicoelasticity: continuum formulation and finite element applications to elastomeric structures. *International journal of numerical methods in engineering*, **39**, 3903-3926.

18. **Holzpfel, G. A. and J. C. Simo** (1996), A new viscoelastic constitutive model for continuous media at finite thermomechanical changes. *International journal of solids and structures*, **33**, 3019-3034.

19. **Kaliske, M.** (2000), A formulation of elasticity and viscoelasticity for fibre reinforced material at small and finite strains. *Computer methods in applied mechanics and engineering*, **85**, 225-243.

20. **Lee, E.H.** (1969), Elastic-plastic deformation at finite strain. *Journal of applied mechanics*, **36**, 1-6.

21. **Le Tallec, P., A. Kaiss, and C. Rahier** (1993), Three dimensional incompressible viscoelasticity in large strains: Formulation and numerical approximation. *Computer methods in applied mechanics and engineering*, **109**, 233-258.

22. **Lin, R.C. and U. Schomburg** (2003), A finite elastic-viscoelastic-elastoplastic material law with damage: theoretical and numerical aspects. *Computer methods in applied mechanics and engineering*, **192**, 1591-1627.

23. **Lin, R.C., W. Brocks and J. Betten** (2006), On the internal dissipation inequalities and finite strain constitutive laws: Theoretical and numerical comparisons. *International journal of plasticity*, **22**, 1825-1857.

24. **Lion, A.** (1996), A constitutive model for carbon black filled rubber: Experimental investigations and mathematical representation. C*ontinuum mechanics and thermodynamics*, **l8**, 153-169.

25. **Lion, A.** (1997a), On the large deformation behavior of reinforced rubber at different temperatures. *Journal of the mechanics and physics of solids*, **45**, 1805-1834.

26. **Lion, A.** (1997b), A physically based method to represent the thermo-mechanical behaviour of elastomers. *Acta mechanica*, **123**, 1-25.

27. **Lubliner, J.** (1985), A model of rubber viscoelasticity. *Mechanics research communications*, **12**, 93-99.

28. **Mullins, L.** (1969), Softening of rubber by deformation. *Rubber chemistry and technology*, **42**, 362-399.

29. **Narasimha Rao, K.V.** *Design of Pnuematic Tyers with Finite Element Analysis*, PhD thesis, IIT Madras, 2005.

30. **Narasimha Rao, K.V., R. Krishna Kumar, P.C. Bohara and R. Mukhopadhyay** (2006), A finite element algorithm for the prediction of steady-state temperatures of rolling tires. *Tire science and technology, TSTCA*, **34**, 195-214.

31. **Nedjar, B.** (2002a), Frameworks for finite strain viscoelastic-plasticity based on multiplicative decompositions part I: Continuum formulations. C*omputer methods in applied mechanics and engineering*, **l91**, 1541-1562.

32. **Nedjar, B.** (2002b), Frameworks for finite strain viscoelastic-plasticity based on multiplicative decompositions part II: Computational aspects. C*omputer methods in applied mechanics and engineering*, **l91**, 1541-1562.

33. **Ogden, R. W.** (1972), Large deformation isotropic elasticity-On the correlation of theory and experiment for incompressible rubberlike solids. *Proceedings of royal society of London, series A, Mathematical and physical sciences*, **326**, 565-584.

34. **Ogden R. W.** *Non-linear elastic deformations*, Ellis Horwood Ltd., 1984.

35. **Reese, S. and P. Wriggers** (1997), a material model for rubber-like polymers exhibiting plastic deformation: Computational aspects and a comparison with experimental results. C*omputer methods in applied mechanics and engineering*, **l48**, 279-298.

36. **Reese, S. and S. Govindjee** (1998a), A theory of finite viscoelasticity and numerical aspects. *International journal of solids and structures*, **35**, 3455-3482.

37. **Reese, S. and S. Govindjee** (1998b), Theoritical and numerical aspects in the thermo-viscoelastic material behaviour of rubber-like polymers. *Mechanics of time-dependent materials*, **1**, 357-396.

38. **Simo, J. C.** (1988), A frame work for finite strain elastoplasticity based on maximum plastic dissipation and the multiplicative decomposition. Part II: Computational aspects. *Computer methods in applied mechanics and engineering*, **68**, 1-31.

39. **Simo, J.C.** (1992), Algorithms for static and dynamic multiplicative plasticity that preserve the classical return mapping schemes of infinitesimal theory. C*omputer methods in applied mechanics and engineering*, **l99**, 61-112.

40. **Simo, J.C., R. L. Taylor and K.S. Pister** (1985), Variational and projection methods for the volume constraint in finite deformation elastoplasticity. C*omputer methods in applied mechanics and engineering*, **51**, 177-208.

41. **Simo, J.C. and T.J.R., Hughes** *Computational Inelasticity*. Springer-Verlag New York, Inc, 1998.

42. **Treloar, L.R.G.** *ThePphysics of Rubber Elasticity*. Third Edition, Clarendon press. Oxford, 1975.

43. **Truesdel, C. and W. Noll** *The Nonlinear Field Theories of Mechanics.* Second edition, Springer-Verlag Berlin Heidelberg New York, 1992.

44. **Weber, G. and L. Anand** (1990), Finite deformation constitutive equations and a time integration procedure for isotropic, hyperelastic-viscoplastic solids. C*omputer methods in applied mechanics and engineering*, **79**, 173-202.

45. **Wineman, A. S., and K. R. Rajagopal** *Mechanical Response of Polymers an Introduction.* Cambridge university press, 2000.

46. **Wu, H.C.** *Continuum Mechanics and Plasticity.* Chapman & Hall/CRC, 2000.

47. **Valanis, K.C**. (1971) A theory of viscoplasticity without a yield surface. *Archive of applied mechanics*, **23**, 517-533.

48. **Valanis, K.C**. (1980) Fundamental consequences of a new intrinsic time measure plasticity as a limit of the endochronic theory. *Archives of mechanics*, **32**, 171-191.

49. **Yeoh, O. H.** (1993), some forms of strain energy function for rubber. *Rubber chemistry and technology*, **66**, 754-771.

50. **Zienkiewicz, O. C. and R. L. Taylor** *The finite element method, volume1*. Fifth Edition, Butterworth Heinemann, 2000.

51. **Zienkiewicz, O. C. and R. L. Taylor** *The finite element method, volume2*. Fifth Edition, Butterworth Heinemann, 2000.

LIST OF PUBLICATIONS BASED ON THE RESEARCH WORK

I. JOURNALS

1. **Aravind Peketi and R. Krishna Kumar,** Development of finite strain viscoelastic-plastic material model (To be communicated).

II. CONFERENCES

1. **Aravind Peketi and R. Krishna Kumar.** A non-linear viscoelastic-plastic constitutive model. *International Conference on Computational, Mathematical and Statistical Methods*, Chennai, January, 2007.